Task 2.2

Title

Infrastructure adaption

Projects (presented on the following pages)

Gestion de sédiments dans les retenues suisses : expériences vécues et défis à relever
Samuel Vorlet, Pedro Manso

Hydro-abrasion at hydraulic structures and steep bedrock rivers
Dila Demiral, Ismail Albayrak, Robert Boes

Storage hydropower potential from dam heightening in Switzerland
Andrin Leimgruber, David Felix, Michelle Müller-Hagmann, Robert Boes

Storage hydropower potential from dam heightening in the cantons of FR, NW, OW, UR, VD and VS
Jule Claire Holland, Samuel Wolf, Hannes Zimmermann, David Felix, Michelle Müller-Hagmann, Robert Boes

Storage hydropower potential from dam heightening in the cantons of BE, TI and SZ
Cecilia Parravicini, Damiano Vicari, Raphael Werlen, David Felix, Michelle Müller-Hagmann, Robert Boes

Storage hydropower potential from dam heightening in the cantons of GL, GR and SG
Marco Baumann, Alain Emmenegger, Andrin Kasper, David Felix, Michelle Müller-Hagmann, Robert Boes

Nucleation of laboratory earthquakes: Implications for EGS induced seismicity
Mateo Acosta, Francois Passelègue, Alexandre Schubnel, Benoit Gibert, Marie Violay

Blocking probability at spillway inlets under driftwood impact
Paloma Furlan, Michael Pfister, Jorge Matos, Anton J. Schleiss

Spatial Impulse Wave Generation and Propagation
Eva Sauter, Frederic Evers, Helge Fuchs, Robert Boes

Impulse waves: run-up behavior and overtopping at dam structures
Fabian, Küttel, Frederic Evers, David Vetsch, Robert Boes

Wave generation by submarine mass failures
Nina Landolt, Frederic Evers, Helge Fuchs, Robert Boes

Influence of tunnel slope on air demand and flow conditions in bottom outlets
Alexander Williams, Benjamin Hohermuth, Lukas Schmocker, Robert Boes

Numerical Simulations of Two-Phase Flow in Bottom Outlets
Matthias Bürgler, Benjamin Hohermuth, David Vetsch, Robert Boes

Les principaux vecteurs d'adaptation d'installations hydroélectriques de montagne en Suisse
Vincent Gaertner, Sabine Chamoun, Pedro Manso

Valorisation des mesures de mitigation des éclusées en systèmes complexes : quelle échelle spatiale privilégier ?

Mathieu Barnoud, Sabine Chamoun, Pedro Manso

SCCER SoE
SWISS COMPETENCE CENTER for ENERGY RESEARCH
SUPPLY of ELECTRICITY

SCCER-SoE Annual Conference 2018

Supported by:
Schweizerische Eidgenossenschaft
Confédération suisse
Confederazione Svizzera
Confederaziun svizra
Swiss Confederation
Innosuisse – Swiss Innovation Agency

Gestion de sédiments dans les retenues suisses : expériences vécues et défis à relever

Schweizerisches Talsperrenkomitee
Comité suisse des barrages
Comitato svizzero delle dighe
Swiss Committee on Dams

Samuel L. Vorlet, Pedro Manso*
Platform of Hydraulic Construction (PL-LCH), École Polytechnique Fédérale de Lausanne (EPFL), Switzerland
**Corresponding author: samuel.vorlet@epfl.ch*

ÉCOLE POLYTECHNIQUE FÉDÉRALE DE LAUSANNE

Contexte de l'étude

La sédimentation est un des problèmes actuels principaux dans les réservoirs en Suisse. Dans un contexte de transition énergétique et de vieillissement des infrastructures, la gestion des sédiments dans les retenues représente un défi majeur pour les exploitants, qui doivent trouver des solutions innovantes pour assurer le rétablissement du transfert des sédiments à travers les réservoirs, tout en limitant les pertes d'eau, en respectant les contraintes légales et les contraintes liées à la production hydroélectrique.
Cette étude vise à illustrer le problème que représente la sédimentation en Suisse ainsi que sa gestion par les divers exploitants. L'objectif est d'obtenir des informations pour catégoriser les retenues sujettes à des problèmes liés aux sédiments.

***Figure 1:** Déposition de sédiments; Giétroz du Fond, 2018*

Méthodes

Une étude a été réalisée auprès de divers exploitants de barrages en Suisse par rapport à la gestion sédimentaire et aux principaux problèmes liés aux sédiments auxquels ils sont confrontés. Un questionnaire a été élaboré au sein du groupe de travail « Purges et Vidanges de Retenues » du Comité Suisse des Barrages (CSB), qui a ensuite été transmis aux exploitants.
Au total, 34 participants ont pris part à l'enquête qui regroupe les résultats concernant 69 retenues en Suisse et permet de mettre en évidence les expériences vécues et les principaux défis à relever au niveau national. Les résultats permettent également de mettre en avant l'importance de la gestion des sédiments pour les retenues en Suisse.

***Figure 2**: Localisation des retenues ayant participé à l'enquête*

Résultats

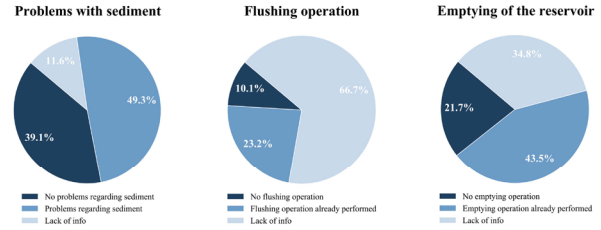

***Figure 3:** Retenues confrontées à des problèmes liés aux sédiments; opérations de purge; vidanges*

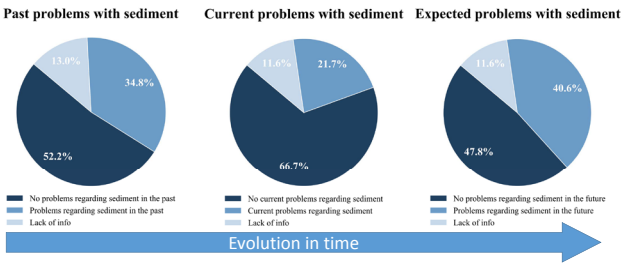

***Figure 4:** Retenues confrontées à des problèmes liés aux sédiments: évolution temporelle*

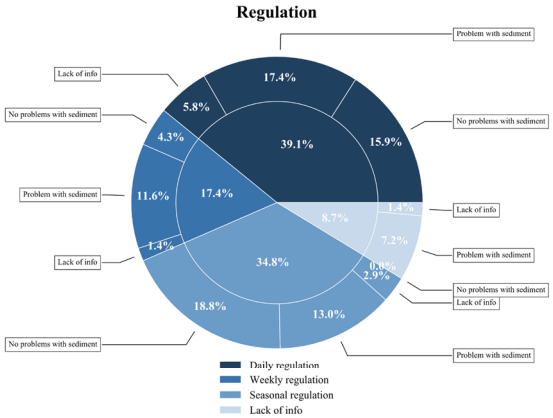

***Figure 5:** Régulation des réservoirs et problèmes liés aux sédiments*

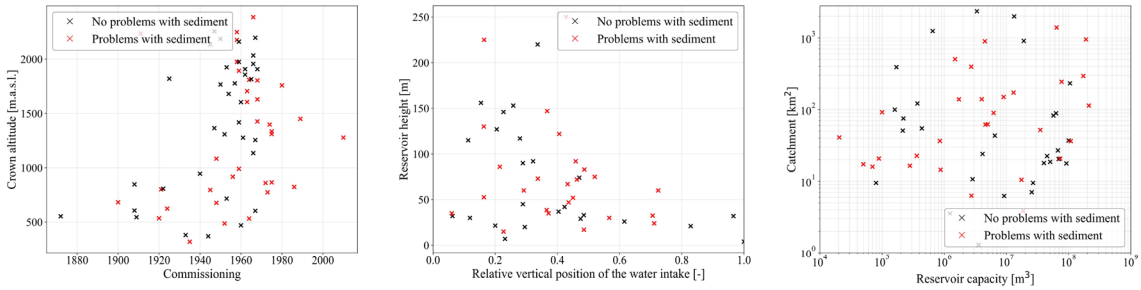

***Figure 6:** Classification des réservoirs en fonction de: l'année de mise en service et l'altitude de la couronne, de la hauteur relative de la prise d'eau et de la hauteur du barrage, de la capacité du réservoir et de la taille du bassin versant; en noir: pas de problèmes avec les sédiments, en rouge: problèmes avec les sédiments*

Conclusions

Les résultats de l'enquête concernant 69 retenues en Suisse montrent que la gestion des sédiments en Suisse représente un défi majeur. A terme, une majorité de retenues sera sujette à des problèmes liés à la sédimentation. De plus, on observe que peu importe l'année de mise en service, l'altitude, la position relative de la prise d'eau, la hauteur du barrage, la capacité du réservoir ou la taille du bassin versant, toutes les retenues peuvent faire face à des problèmes liés aux sédiments.
L'expérience vécue des exploitants doit permettre de mettre en place une uniformisation des mesures concernant la gestion des sédiments dans les retenues en Suisse. Par la suite, il sera nécessaire d'intégrer un plan de gestion des sédiments dans les directives sécuritaires et environnementales des barrages, afin de gérer au mieux les problèmes liés à la sédimentation dans les décennies à venir.

Remerciements

Cette enquête a été réalisée dans le cadre du groupe de travail «Purges et Vidanges de Retenues» du Comité Suisse des Barrages (CSB). Les remerciements sont adressés à tous les membres du groupe de travail (P. Manso, A. Baumer, N. Bretz, D. Ehrbar, G. Federer, M. Müller, M. Nitsche, A. Ricciardi, T. Rüesch, J. Stamm, T. Ziegler) ainsi qu'à tous les exploitants ayant répondu aux questionnaires.

SCCER SoE
SWISS COMPETENCE CENTER for ENERGY RESEARCH
SUPPLY of ELECTRICITY

SCCER-SoE Annual Conference 2018

Supported by:
Schweizerische Eidgenossenschaft
Confédération suisse
Confederazione Svizzera
Confederaziun svizra
Swiss Confederation
Innosuisse – Swiss Innovation Agency

Hydro-abrasion at hydraulic structures and steep bedrock rivers

Dila Demiral, Ismail Albayrak, Robert Boes
ETH Zurich, Switzerland

Motivation and objectives

Sediment transport from glacier basins, rivers and waterways, and reservoir sedimentation worldwide have strongly increased under the strong impact of climate change. As a consequence, high transport rates of bed load particles combined with high flow velocities cause severe abrasion such as (I) hydro-abrasion at hydraulic structures, such as Sediment Bypass Tunnels (SBTs) and Sediment Flushing Channels (SFCs) (Fig 1), and (II) bedrock incision in high-gradient mountain streams (Fig 2). Despite the large number of studies mainly in alluvial channels, only few exist for steep bedrock rivers and non-movable bed open channels. However, their applicability is still in question for highly supercritical flow due to the lack of information on the physical processes of turbulent flow characteristics, bed load particle motion, and abrasion and their interrelations. The proposed project aims at filling the research gaps by a systematic laboratory investigation.

Fig 1. Hydro-abrasion at Palagnedra SBT (Photo: VAW, ETH)

Fig 2. Bedrock incision at Ukak River, Alaska, US

The main objectives of this study are to: (1) investigate the mean and turbulent flow characteristics in supercritical narrow open channel flows (i.e. channel width to water depth, b/h < 3-5) over fixed and abraded-fixed beds, (2) investigate single and multi-particle motions over fixed and abraded-fixed beds, (3) determine the hydro-abrasion depth and pattern for a range of polyurethane foams and erodible mortars, (4) develop a mechanistic hydro-abrasion model to forecast hydro-abrasion at both laboratory and prototype scales.

Experimental setup and research tasks

The experiments of the present study are conducted in a b = 20 cm wide, h = 50 cm deep and l = 13.50 m long laboratory flume (Fig 3). The flume bottom is concrete lined and the bed slope is S_0 = 0.01.

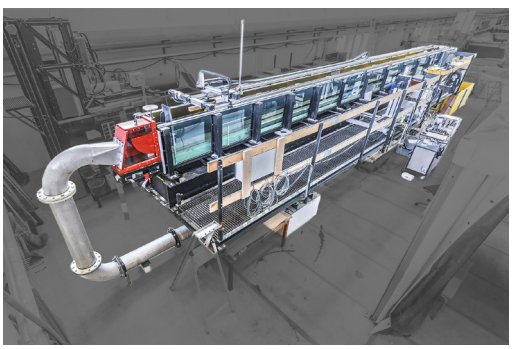

Fig 3. Experimental flume (Photo: VAW, ETH)

To meet the objectives, the project is divided into four tasks, namely Task A, B, C and D.

In Task A, velocity measurements were conducted using a 2D Laser Doppler Anemometer (LDA) to determine the cross-sectional mean flow velocities and turbulence intensities, bed and Reynolds shear stresses on different flow conditions (i.e. b/h_0 = 1, 1.33 and 2; and F=2, 3 and 4).

In Task B, high speed video recordings of particles are made to determine the particle transport mode, trajectory, velocity, and impact energy under various hydraulics conditions for a range of particle differing in size, shape and hardness.

In Task C, the goal is to systematically investigate the effects of the sediment size, hardness, and transport rate on hydro-abrasion of different types of bed lining materials (foam and erodible mortar) under various hydraulic conditions.

Task D focuses on the development of an abrasion prediction model based on the data from Tasks A, B and C.

First results

Figure 4 shows the contour lines of mean streamwise (U) and vertical (W) velocities normalized by the max. streamwise velocity, U_{max} together with the sketches of the secondary current cells for b/h_0 = 2 and F = 2, 3 and 4. From the streamwise and vertical velocity distributions, a pair of surface and a pair of corner vortices called 'secondary currents' were identified at each side of the flume, resulting in a 3D flow pattern. The streamwise velocities are symmetrical and the maximum flow velocity occurs below the surface around z/h = 0.5-0.6, which is so-called 'velocity dip phenomenon' (Fig 4 a-c) . Additionally, vertical contour plots show a quasi-symmetrical flow pattern with strong downward flows below the water surface at the flume center (y/h = 0). The results show that the secondary currents are not affected by the Froude number. These currents not only affect the mean flow characteristics but also cause a redistribution of bed and Reynolds shear stresses, which plays an important role in sediment transport, and hence the hydro-abrasion mechanism.

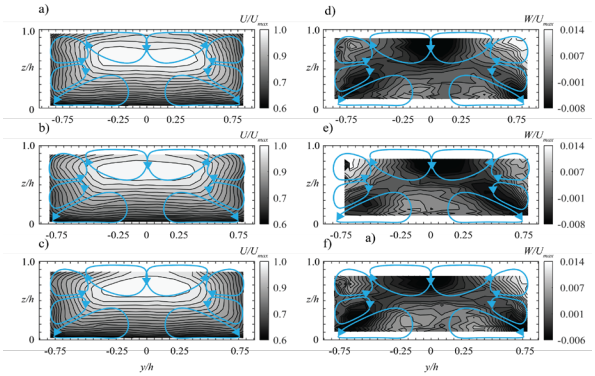

Fig 4. Contour plots of streamwise and vertical flow velocities for h_0 = 10 cm and F = 2 (a-d), 3 (b-e) and 4 (c-f).

Outlook

The measurements and data analysis in Task A were completed. The experiments in Task B are on-going. Task C will be conducted in autumn 2018 while Task D will be done in 2019. The outputs of this project will contribute to design and sustainable use of hydraulic structures i.e. SBTs, SFCs and modelling of bedrock incision in steep rivers and landscape evolution exposed to heavy sediment loads.

SCCER SoE
SWISS COMPETENCE CENTER for ENERGY RESEARCH
SUPPLY of ELECTRICITY

SCCER-SoE Annual Conference 2018

Supported by:
Schweizerische Eidgenossenschaft
Confédération suisse
Confederazione Svizzera
Confederaziun svizra
Swiss Confederation
Innosuisse – Swiss Innovation Agency

Storage hydropower potential from dam heightening in Switzerland

Andrin Leimgruber, David Felix, Michelle Müller-Hagmann, Robert Boes – VAW ETH Zürich

Introduction

In winter, the domestic electricity production in Switzerland has not been sufficient to cover the demand since more than 10 years. With the planned shutdown of the nuclear power plants according to the Swiss Energy Strategy 2050, the need for imports of electric energy in winter will increase. Existing storage hydropower plants (HPPs) could provide more electric energy in winter if their headwater storages (reservoirs) would be enlarged by dam heightening (Schleiss 2012).
This study aimed firstly at estimating the potentially achievable additional storage volumes in Switzerland and the corresponding amount of electricity production which could be shifted from summer to winter. Secondly, a case study at the Griessee was conducted to investigate examples of site-specific aspects.

Part I: Potential study of dam heightening in Switzerland

Methods

Dam heightening options by 5%, 10% and 20% of the existing dam heights were roughly analyzed for the 38 largest HPP reservoirs in Switzerland. The options were assessed based on multiple criteria including technical, ecological, economical and social aspects. The future additional reservoir area, the dam and the HPP system were considered.
The additional storage volumes and the corresponding energy production which can be additionally transferred from summer to winter were estimated for two scenarios. In Scenario 1 the most promising heightening options were identified (16 dams). In scenario 2, also further heightening options with a smaller probability of realization were considered (totally 29 dams).

Results

The electricity production which could be additionally transferred from summer to winter is estimated as **1.7** and **2.8 TWh** per year for Scenario 1 and 2, respectively. The contributions of the reservoirs are shown in Figure 1. In both scenarios, the achievable potential depends significantly on the feasibility of specific heightening projects at single large reservoirs (e.g. Lac des Dix impounded by the Grande Dixence dam, Emosson, Grimsel and Oberaar).

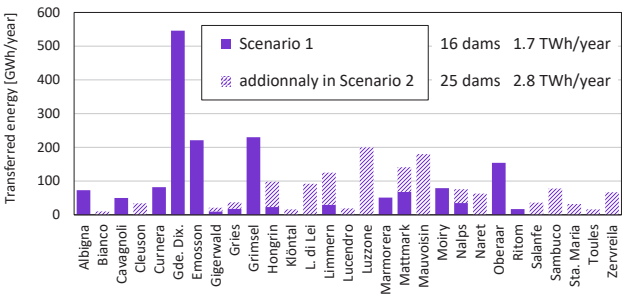

Fig. 1: Annual electricity which could be additionally transferred from summer to winter after dam heightenings

Conclusion

Dam heightening with the corresponding adaptation of HPP operation has the potential to considerably reduce the need for electricity imports in winter, which are presently about 3 TWh/year and could increase up to 10 TWh/year (Piot 2014).
It is recommended to study dam heightening options as well as the required adaptation of HPPs and neighbouring infrastructures in more detail. Moreover it is recommended to review the energy policy to set additional incentives for more winter electricity production if a high degree of domestic production is aimed at in the future.

Part II: Dam heightening at Griessee (Case study)

Existing HPP

The Griessee is located in the canton of Valais close to the Nufenen pass. The full supply level of this reservoir with a storage capacity of 18.4 Mio. m³ is 2386.5 m a.s.l. The arch gravity dam was built in 1966 and is 60 m high (Fig. 2). The water of the Griessee is turbined first in Altstafel and then in several HPP stages of the Maggia cascade. The elevation difference down to the Lago Maggiore (193 m a.s.l.) is almost 2200 m. About 5 kWh are generated from each m³ of water.

Fig. 2: Arch gravity dam Gries

Dam heightening alternatives

Five heightening alternatives by 5%, 10% and 20% of the existing dam height were investigated considering two structural options (Table 1). From an energy-policy point of view and to increase the operational flexibility, Alternative 3 was preferred in this study despite the relatively high specific costs.

Alternative	Heightening [m]	Storage capacity [Mio m³]	Structural option for reinforcement	Production shifted to winter [GWh]	Add. specific costs [CHF/kWh]
1.1	3	20.8	Crown	11.4	0.012
1.2	3	20.8	Downstream face	11.4	0.12
2.1	6	22.2	Crown	18.1	0.016
2.2	6	22.2	Downstream face	18.1	0.12
3	12	26.2	Downstream face	37.3	0.09

Because the inflows are not sufficient to fill the enlarged reservoir every year, a new compensation basin is proposed, from which additional water can be pumped up to the Griessee (Fig. 3). Figure 4 shows the cross section of the dam at the location of the spillway.

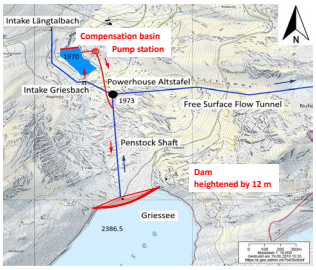

Fig. 3: Map of the hydropower scheme

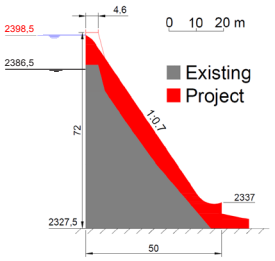

Fig. 4: Cross section of the dam

Conclusion

It is recommended to further investigate the option of heightening the Gries dam because the impact on the additional reservoir area is relatively low and the specific energy is high. However, due to the rather small storage volume, the additional winter energy production is relatively low compared to that of major Swiss HPP reservoirs.

References

Schleiss, A. (2012): Talsperrenerhöhungen in der Schweiz: Energiewirtschaftliche Bedeutung und Randbedingungen, *Wasser Energie Luft* 104 (3), 199-203.
Piot, M. (2014): Bedeutung der Speicher- und Pumpspeicherkraftwerke für die Energiestrategie 2050 der Schweiz, *Wasser Energie Luft* 106 (4), 259-265.

SCCER SoE
SWISS COMPETENCE CENTER for ENERGY RESEARCH
SUPPLY of ELECTRICITY

SCCER-SoE Annual Conference 2018

Supported by:
Schweizerische Eidgenossenschaft
Confédération suisse
Confederazione Svizzera
Confederaziun svizra
Swiss Confederation
Innosuisse – Swiss Innovation Agency

Storage hydropower potential from dam heightening in the cantons of FR, NW, OW, UR, VD and VS

Jule C. Holland, Samuel Wolf, Hannes Zimmermann, David Felix, Michelle Müller-Hagmann, Robert Boes – VAW ETH Zürich

Introduction

Since 2003, the Swiss demand for electric energy in the winter semester (about 31 TWh) has exceeded the domestic production by 3 TWh on average (BFE 2016). With the planned phase-out from nuclear energy the needs for imports could increase to up to 10 TWh (Piot 2014).
The storage hydropower plants (HPPs) are important for the electricity supply, particularly in winter. This contribution can be increased if reservoirs (storage lakes) are enlarged by dam heightening.
The present study comprises two parts: Firstly, an analysis of the energy potential of dam heightening at the existing HPP reservoirs in the Swiss cantons of Fribourg, Nidwalden, Obwalden, Uri, Vaud and Valais. These HPPs provide nowadays 49% of the Swiss electricity in winter. Secondly, heightening options for the Sera arch dam (Fig. 1), located in the Zwischbergen valley in the canton Valais, were investigated as a case study in collaboration with Alpiq Group SA.

Fig. 1: Aerial view of the Sera reservoir (left) and downstream view on Sera arch dam

Part I: Energy potential study

Various options to heighten the dams in the mentioned cantons by 5, 10 or 20 percent were assessed based on multiple criteria. These considered the additional areas occupied by the extended reservoirs, the dams with their appurtenant structures and the HPP systems. In Scenario 1 the most promising options were considered, in Scenario 2 also options with a lower probability of realization.

Results

It was estimated that the **active storage volumes** of the reservoirs in the considered cantons could be increased by **180** or **440 Mio. m³** in Scenario 1 or 2, respectively. This corresponds to 12 to 28% of the existing active storage. With enlarged reservoirs, **0.5** to **1.5 TWh** of **electricity production** could be additionally shifted from summer to **winter** (Fig. 2). The electricity production in winter would hence increase by 7 to 20% in the considered cantons. These results strongly depend on single large reservoirs (e.g. heightening of the Grande Dixence dam by 10% makes up 520 GWh in Scenario 2).

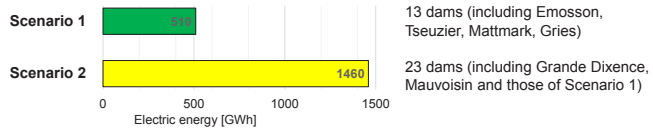

Fig. 2: Potential transfer of electricity production from summer to winter with enlarged reservoirs due to dam heightening in the cantons of FR, NW, OW, UR, VD and VS

Conclusions and Outlook

Heightening of existing dams with the corresponding HPP adaptations has the potential to contribute significantly to a higher electricity production in winter. Moreover, larger storage volumes increase the operational flexibility of HPPs which is also important to reach the goals of the *Energy Strategy 2050.* It is recommended to study dam heightening options in more detail and to introduce additional incentives to foster the increase of storage capacities of HPPs.

References

BFE (2016): Schweizerische Elekrizitätsstatistik, Bundesamt f. Energie.
Piot, M. (2014): Bedeutung der Speicher- und Pumpspeicherkraftwerke für die Energiestrategie 2050 der Schweiz, *Wasser Energie Luft* 106 (4), 259-265.

Part II: Heightening of Sera dam (case study)

Various options to heighten the Sera arch dam and its full supply level by 3 or 6 m were investigated, also based on previous studies. Preference was given to the option of 6 m, keeping the unregulated spillway.

Results

Previous studies and structural analysis by means of the Trial Load Method showed that the existing arch **dam** can be heightened from 19.5 to 26.4 m without any reinforcement on its downstream face (Fig. 3). It is proposed to increase the vertical distance between the spillway crest and the bridge to achieve a larger freeboard for driftwood during extreme floods.
As a consequence of the raised full supply level, the main water adduction tunnel needs to be adapted and the intermediate **intake** in the Laggintal needs to be rebuilt at a higher level. The upper chamber of the **surge tank** needs to be enlarged. The cantonal **road** along the reservoir, the **substation** and the **inlet** to the **sediment bypasss tunnel** need to be adapted and relocated (Fig. 4).

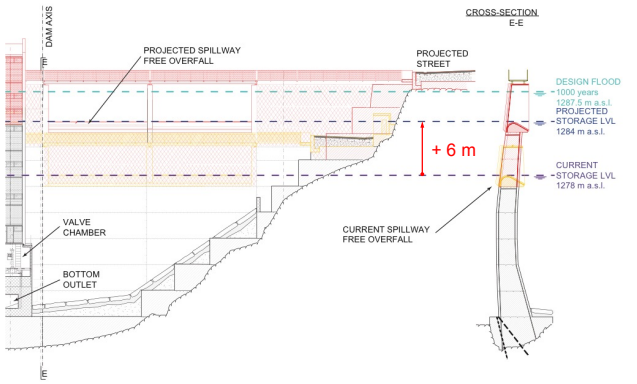

Fig. 3: Downstream view of the proposed dam heightening (left) and cross-section (right) (drawings modified from Lombardi SA)

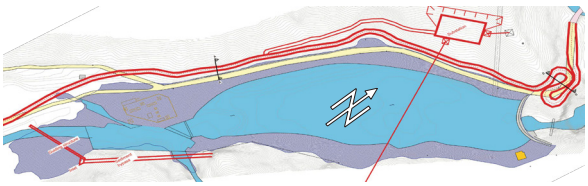

Fig. 4: Schematic plan view of Sera reservoir with full supply level raised by 6 m and corresponding adaptations (modified from SPI Schmidhalter Partner Ingenieure AG)

Due to the higher reservoir water levels, the annual production would increase by **1.6 GWh**, while **0.2 GWh** can be additionally transferred from to the summer to the winter semester.

The project costs were estimated as 18.8 Mio CHF. With an interest rate of 2 % and an amortization duration of 80 years, the specific costs of the additional production are 0.3 CHF/kWh, which is above average market conditions. The specific additional cost to shift the 0.2 GWh from summer to winter would even be 2.1 CHF/kWh.

Conclusions and Outlook

The heightening of the Sera dam cannot be economically justified by the increased electricity production in winter. However, the project increases the operational flexibility in the winter months. The adaptation of existing structures such as roads, intakes and surge tanks strongly affect the economic viability of dam heightening projects.

Acknowledgements

The collaboration with Alpiq Group SA is greatly appreciated.

SCCER SoE
SWISS COMPETENCE CENTER for ENERGY RESEARCH
SUPPLY of ELECTRICITY

SCCER-SoE Annual Conference 2018

Supported by:
Schweizerische Eidgenossenschaft
Confédération suisse
Confederazione Svizzera
Confederaziun svizra
Swiss Confederation
Innosuisse – Swiss Innovation Agency

Storage hydropower potential from dam heightening in the cantons of BE, TI and SZ

Cecilia Parravicini, Damiano Vicari, Raphael Werlen, D. Felix, M. Müller-Hagmann, R. Boes - VAW, ETH Zürich

Introduction

Since 2003 the Swiss electricity production in winter is not sufficient to cover the demand. With the planned phase-out from nuclear power according to the *Swiss Energy Strategy 2050*, this deficit will increase. Extending the storage capacity of hydropower plants (HPPs) by heightening of existing dams could contribute to reduce this deficit.
This work aimed firstly at exploring the potential of dam heightening for three Cantons in southern and central Switzerland and secondly at investigating examples of site-specific challenges in a case study at Sambuco dam in the canton of Ticino (Fig. 1).

Fig. 1: Downstream view of Sambuco arch gravity dam.

Part I: Potential study

For 25 reservoirs with a volume of >1 Mio. m³ in the cantons of BE, TI and SZ, dam heightening options by 5%, 10% and 20% of the original dam heights were assessed based on eight criteria. These involved technical, social, ecological and economical aspects. The investigated HPPs contribute currently to 21% of the production from Swiss storage hydropower. In Scenario 1 the most promising options were considered, in Scenario 2 also options with a lower probability of realization.

Results

Figure 2 shows the electricity production which could be additionally shifted from summer to winter in both scenarios. Currently, the investigated HPPs generate annually 4.6 TWh, of which 2.2 TWh in winter. In Scenario 2, the electricity production in winter could hence be increased by 36%.

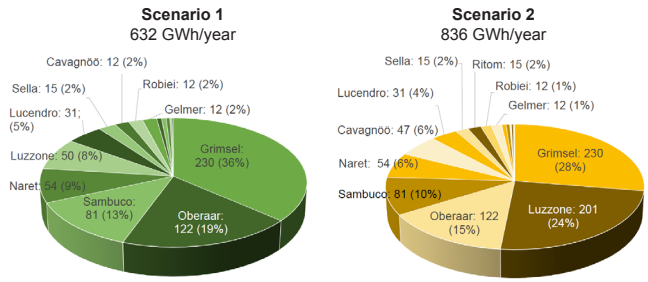

Fig. 2: Estimated electricity production transferred from summer to winter in the cantons of TI, BE and SZ for both scenarios. The absolute numbers are GWh per year, the percentages indicate the contribution to the total of the respective scenario.

The major contribution of 230 GWh per year from Grimsel reservoir results from an assumed 20%-heightening of the Spitallamm arch dam. This correspond to a heightening of 23 m, as studied earlier by the HPP operator (Kraftwerke Oberhasli AG).

Conclusion

If the estimates from the investigated cantons are extrapolated to whole Switzerland, the results are similar to those of previous studies (e.g. Schleiss 2012). Dam heightening has the potential to significantly increase the Swiss electricity production in winter.

Part II: Case Study Sambuco Dam

The Sambuco dam is located upstream of the Peggia HPP and is part of the Maggia cascade. The 130 m heigh arch gravity dam built in 1956 has a storage capacity of 63 Mio. m³. The elevation difference between its full supply level (1461 m a.s.l.) and the Lago Maggiore at the end of the cascade is 1268 m. The current electricity production at Peggia is about 85 GWh per year, of which 60 GWh (71%) in winter.

Dam heightening option

A dam heightening of 10 m, i.e. 7 % of the current dam height, was chosen considering mainly the estimated reserves in the dam's load-bearing capacity and the average natural inflows (93 Mio. m³/a). The cross section of the proposed concrete structure on the existing dam crest is shown in Figure 3. The active storage volume would increase by 15%. The additional electricity production in winter is estimated as 26 GWh taking into account the whole HPP cascade (of which 9 GWh in Peccia HPP).
The dam's spillway and the upper chamber of the surge tank in connection with a water adduction tunnel have to be adapted according to the higher full supply level. The existing local road along the lake (3.3 km) has to be rebuilt at a higher elevation or replaced by a tunnel (less natural hazards and landscape impact). The estimated total costs of the project are either 72 or 195 Mio. CHF for the open road or tunnel alternative, respectively. The costs of the road adaptation make up 37% or even 58% (without or with tunnel) of the total project costs. With the first road adaptation option, the specific costs per meter dam heightening and per m³ of dam concrete are slightly higher than those of reference projects.
The specific costs to shift the 26 GWh from summer to winter are estimated as 0.068 CHF/kWh. This means that the price of this winter electricity would be considerably higher than average market prices.

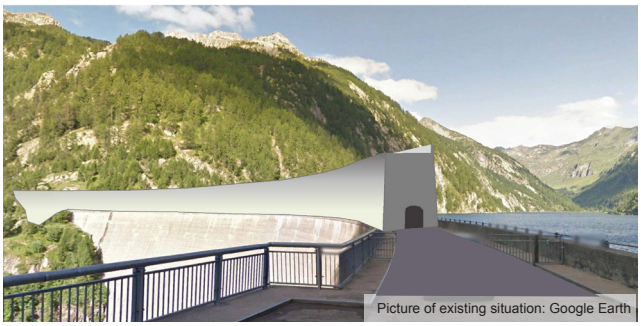

Fig. 3: Visualization of heightening the Sambuco dam by 10 m (during construction).

Conclusions

Extending the reservoirs of existing storage HPPs in Switzerland by moderate dam heightening has the potential to considerably increase the electricity generation in winter. However, the economic viability of such projects depends on the regulatory and market conditions in the future. The case study Sambuco shows that local peculiarities such as existing roads might strongly affect the feasibility of such projects, requiring more in-depth studies.

Acknowledgements

We thank OFIMA for having provided information and drawings on the existing Sambuco dam an the HPP scheme.

References

Schleiss, A. (2012): Talsperrenerhöhungen in der Schweiz: energiewirtschaftliche Bedeutung und Randbedingungen. *Wasser Energie Luft 104(3)*.
BFE (2016): Schweizerische Elekrizitätsstatistik, Bundesamt für Energie.
BFE (2017): Schweizerische Wasserkraftstatistik, Bundesamt für Energie.

SCCER SoE
SWISS COMPETENCE CENTER for ENERGY RESEARCH
SUPPLY of ELECTRICITY

SCCER-SoE Annual Conference 2018

Supported by:
Schweizerische Eidgenossenschaft
Confédération suisse
Confederazione Svizzera
Confederaziun svizra
Swiss Confederation
Innosuisse – Swiss Innovation Agency

Storage hydropower potential from dam heightening in the cantons of GL, GR and SG

Marco Baumann, Alain Emmenegger, Andrin Kasper, D. Felix, M. Müller-Hagmann, R. Boes - VAW, ETH Zürich

Motivation

In the last 10 years, on average 3.5 TWh of electric energy were net imported to Switzerland in every winter (BFE 2016). With the planned phase-out from nuclear power according to the Swiss *Energy Strategy 2050*, the need for electricity imports is estimated to increase to about 10 TWh per winter (Piot 2014).
One possibility to cover this seasonal deficit in domestic production is to enlarge the storage reservoirs of hydropower plants (HPPs). Because the construction of new reservoirs is rather difficult, the heightening of already existing dams is an attractive option. According to previous studies (BFE 2004, Schleiss 2012) an additional electricity production between 0.7 TWh and 2.5 TWh per winter could be reached by this way.

Part I: Potential study in eastern Switzerland

Dam heightening options by 5%, 10% and 20% of the original dam heights were assessed for 24 dams in the cantons of GL, GR and SG based on eight criteria involving technical, social, ecological and economical aspects. In Scenario 1 the most promising options were considered, in Scenario 2 also options with a lower probability of realization.

Results

Figure 1 shows the locations of the reservoirs at which a dam heightening is proposed in the two scenarios. Figure 2 shows the additional storage volumes and the electricity production which could be additionally shifted from summer to winter in Scenario 2. Heightening of 15 dams would increase the electricity production in winter by 600 GWh, of which 500 GWh would come from the largest six reservoirs. In Scenario 1, heightening of six dams would lead to additional 220 GWh in winter.

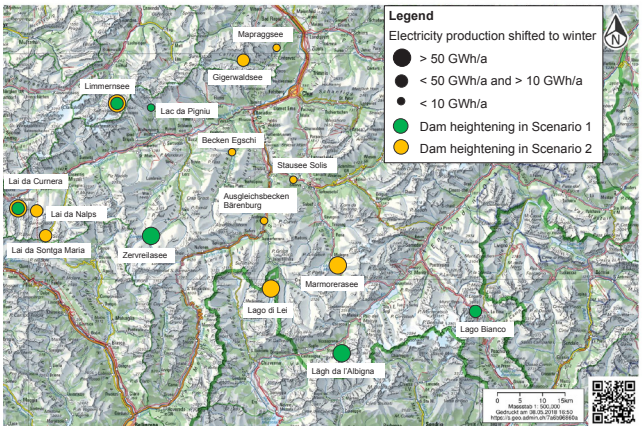

Fig. 1: Location of analysed reservoirs in the two scenarios.

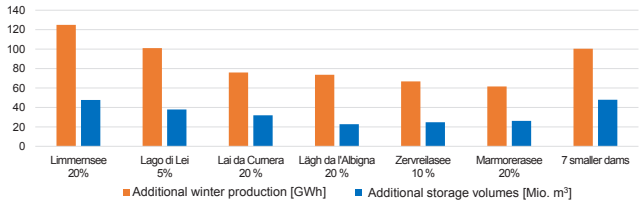

Fig. 2: Additional electricity production in winter and storage volumes in Scenario 2. The percentages indicate the dam heightenings relative to the original dam heights.

Conclusion

If the estimates from the investigated cantons are extrapolated to whole Switzerland, the results are similar to those of previous studies (e.g. Schleiss 2012 and BFE 2004). Dam heightening has the potential to significantly increase the Swiss electricity production in winter.

Part II: Case Study Marmorera Dam

For the 91 m high Marmorera earthfill dam in the Canton of Grisons, Switzerland, various heightening alternatives were considered. The required adaptation works were identified as a function of the extent of dam heightening and the corresponding raise of the full supply level. The considered elements include the dam, its spillway, the water adduction Flix, the surroundings of the lake and the Julier pass road, as well as the surge tank of the HPP Tinizong. The dam heightening alternatives and their key figures are summarized in Table 1.

Tab. 1: Investigated dam heightening alternatives with key figures.

	Project Costs	Annual payment	Additional winter production	Specific costs
	[Mio.CHF]	[kCHF/a]	[GWh/a]	[Rp./kWh]
Alternative +3 m	7.9	198	10.5	**1.9**
Alternative +8 m	58.6	1'473	28.8	**5.1**
+8 m (excl. tunnel)	19.6	492	28.8	1.7
Alternative +11m	87.5	2'201	40.4	**5.4**
+11 m (excl. tunnel)	24.5	615	40.4	1.5

For the alternative “+3 m” the additional cost per kWh transferred from summer to winter are the lowest. This alternative was hence preferred for economical reasons, although a higher electricity production in winter would be favourable from a national energy-policy point of view.
For the alternatives “+8 m” and “+11 m”, major adaptions on the Julier pass road are required mainly in the region of the dam. A new road tunnel is proposed leading to relatively high costs but also to better protection against natural hazards. If the tunnel would be paid partly by public means, dam heightening by 8 or 11 m would become more economic.

Alternative +3 m

Tab. 2: Key figures of alternative +3 m

	Existing	Project	
Dam height	91	94	[m]
Hydraulic head	1061	1064	[m]
Lake surface area	1.4	1.43	[km²]
Storage capacity	61.4	65.7	[Mio. m³]
Energy equivalent	146	157	[GWh]

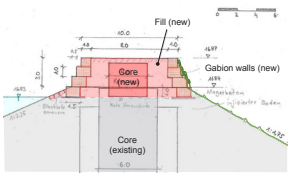

Fig. 3: Cross section of the dam

The following elements would need to be modified: The dam crest (Fig. 3 and item 1 on Fig. 4), the Julier pass road in the region of the dam (item 2 on Fig. 4), the spillway (item 3 on Fig. 4), the water adduction Flix (outlet is item 4 on Fig. 4), the bridge south of the lake (item 5) and finally the surge tank (downstream in the North of Fig. 4).

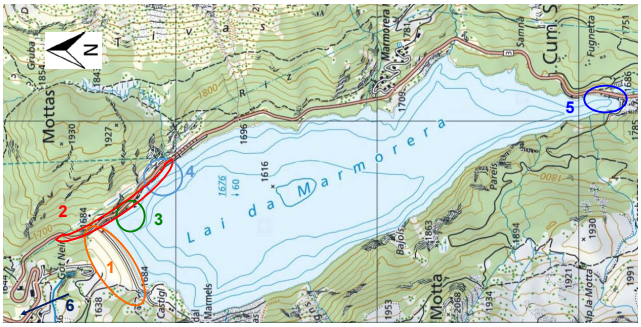

Fig. 4: Map of the Marmorera lake with modifications for dam heightening by 3 m

References

Schleiss, A. (2012): Talsperrenerhöhungen in der Schweiz: energiewirtschaftliche Bedeutung und Randbedingungen. *Wasser Energie Luft 104(3)*.
BFE (2004): Ausbaupotenzial der Wasserkraft. *Studie der Electrowatt-Ekono.*
BFE (2016): Schweizerische Elekrizitätsstatistik, Bundesamt für Energie.
Piot, M. (2014): Bedeutung der Speicher- und Pumpspeicherkraftwerke für die Energiestrategie 2050 der Schweiz, Wasser Energie Luft 106 (4), 259-265.

Nucleation of laboratory earthquakes: Implications for EGS induced seismicity

M.Acosta[1], F.Passelègue[1], A.Schubnel[2], B.Gibert[3], M.Violay[1]*

[1]EPFL, LEMR, Lausanne, Switzerland; [2]Laboratoire de Géologie, CNRS, UMR, ENS, Paris, FR.; [3]Géosciences Montpellier, Université de Montpellier, Montpellier, FR.

*Author for correspondence: mateo.acosta@epfl.ch.

1- Abstract

Recent seismological observations highlighted that both aseismic silent slip or foreshock sequences can precede large earthquake ruptures (Tohoku-Oki, 2011, Mw 9.0; Iquique, 2014, Mw 8.1; Illapel, 2015, Mw 8.3). However, the influence of pore fluid pressure level on the earthquake nucleation behaviour remains poorly understood. Here, we report for the first time, experimental results regarding the nucleation of stick-slip instabilities (laboratory proxies for earthquakes) conducted on Westerly Granite saw-cut samples. Experiments were conducted under stress conditions representative of the upper continental crust, i.e confining pressures from 50 to 125 MPa; fluid pressures (water and argon) ranging from 0 to 45 MPa; and temperatures ranging from 25 to 500˚C.

In dry conditions, we observe that slip evolves exponentially up to the main instabilities and is escorted by an exponential increase of acoustic emissions. With pressurized fluids, precursory slip evolves first exponentially then switches to a power law of time. There, precursory slip remains silent, independently of the fluid pressure level. The amount of precursory slip (u_{prec}) depends on both fluid pressure and initial shear stress. While increasing the initial shear stress leads to larger precursory slip, increasing the fluid pressure seems to reduce the amount of precursory slip leading to instabilities. Independently of the fluid pressure level, we demonstrate that the amount of precursory energy density ($\tau^* u_{prec}$) released prior to the mainshock (the energy dissipated during the precursory stage) scales linearly with the energy density dissipated during the co-seismic stage ($(\tau_f + \Delta\tau/2)^* u_{coss}$). These results suggest that the intensity of the precursory stage is a function of the strength of the asperity which is eventually going to rupture.

Our experimental observations imply that the initial background stress and the pore fluid pressure level control the intensity and the nucleation behaviour of the fault. Such observation indicates that (i) that the presence of foreshock sequences is not systematic during earthquake nucleation and seems attenuated in presence of water, (ii) large ambient pore fluid pressure could reduce the intensity and the duration of the precursory stage.

2- Experimental set-ups

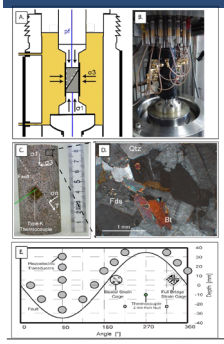

2.1 – Oil loading triaxial apparatus

Fig.1 Experimental set-up at ENS Paris.
A. Oil loading triaxial apparatus.
B. Picture of the experimental sample in the machine.
C. Intact Westerly Granite sample (80 mm length and 40 mm diametre) showing the fault orientation, stresses in the sample and instruments used.
D. Map of the instruments used.

HIGHLIGHTS

- *Upper crustal stress conditions (down-to ~7km depth).*
- *Allows for wide instrumentation (15 Piezo-electric sensors, 4 near-fault strain gages, 1 type-K thermocouple).*
- *High frequency AE and strain (up to 10 MHz sampling frequency).*

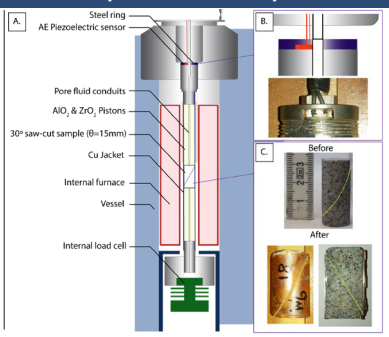

2.2 – High Pressure-High Temperature Paterson rig.

Fig.2 Experimental set-up at Géosciences Montpellier.

A. High Pressure – High temperature Paterson rig. Confining pressure is argon gaz.
B. Detail on the installation of the Acoustic emission sensor located on the top piston 18 cm away from the sample.
C. Intact Westerly Granite sample (32 mm length and 15 mm diametre) showing the fault orientation.
D. Samples after deformation.

HIGHLIGHTS

- *Upper crustal stress and **temperature** conditions (down-to ~10km depth).*
- *Acoustic Emission monitoring.*

3- Experimental results

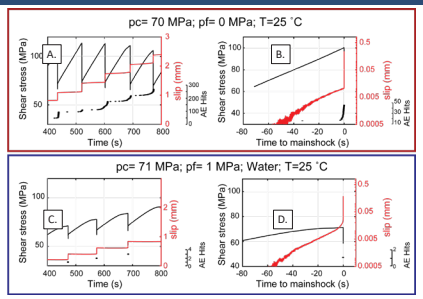

Fig.3. Experimental results from room temperature experiments.

A. Shear stress, fault **slip** and **AE** arrivals evolution on **time** for a **DRY** Experiment (pc=70 MPa). **B. Fluid** pressurized Experiment (pc=71 MPa, pf=1 MPa). **C.** Precursory evolution of **shear stress** (black), corrected **slip** (red in log scale) , and AE arrivals (black dots) on time prior to the mainshock for one event of the **DRY** experiment (pc= 70 MPa). **D.** same as C. for **Fluid** pressurized experiment at pf= 1 MPa.

HIGHLIGHTS

- *Water fluid pressure promotes "silent" aseismic slip.*
- *Precursory slip behavior can be very different depending on fault conditions*

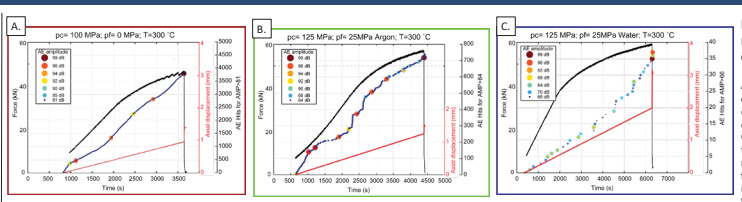

Fig.4 Experimental results from HP-HT experiments.

A. Axial force, axial **displacement** and **AE** arrivals evolution on **time** for a **DRY** experiment (pc= 100 MPa). Circle size and color correspond to the absolute energy from the recorded waveform. **B. Argon fluid** pressurized Experiment (pc=125 MPa, pf= 25 MPa). **C. Water fluid** pressurized Experiment pc=125 MPa, pf= 25 MPa).

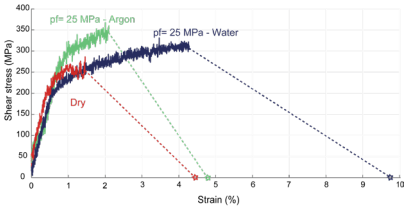

Fig.5 Stress strain evolution from HP-HT experiments.

Red curve corresponds to **DRY** experiment at pc= 100 MPa.
Green to **Argon** fluid pressurized experiment at pc= 125 MPa and pf= 25 MPa.
Blue to **Water** fluid pressurized experiment at pc= 125 MPa and pf= 25 MPa.

HIGHLIGHTS

- *Precursory and and co-seismic strain are longer in presence of water than with argon gas and dry conditions*

4.2 – Energy dissipation during laboratory earthquakes.

Fig.7. Energy spent during laboratory earthquakes.

A. Schematic of shear stress as function of fault slip during the seismic cycle. The shaded areas correspond to what we define as "Precursory Energy" and "Co-seismic Energy". The latest corresponds to the Fracture Energy in the case of a linear slip-weakening case.

B. Co-seismic Energy versus Precursory energy for all stick-slip events at room temperature with additional data from other studies on sawcut and intact rock. Colorbar shows static fault shear strength.

C. Co-seismic Energy versus Precursory energy for OUR stick-slip events at room temperature. Colorbar accounts for pf.

HIGHLIGHTS

- *Co-seismic Energy scales linearly with precursory energy.*

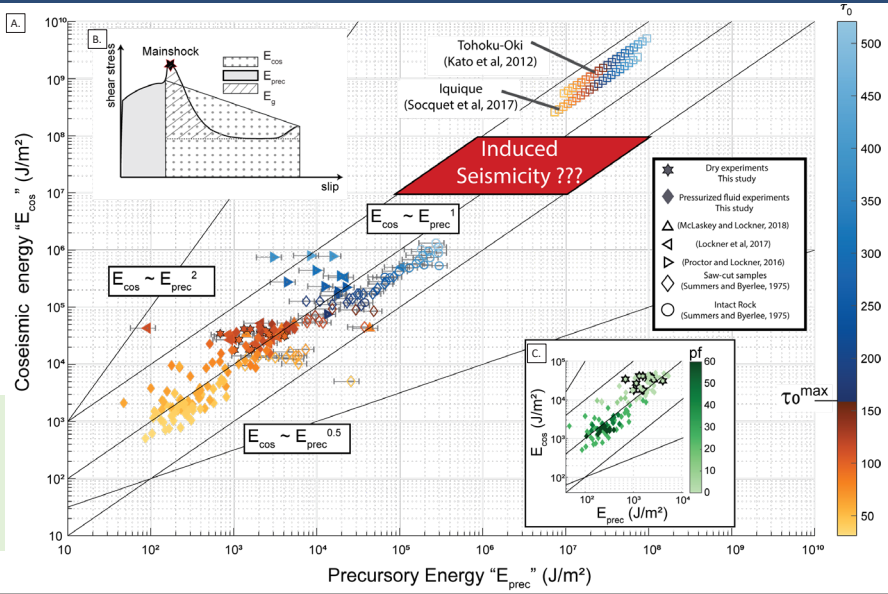

5- Conclusions

- **Water fluid pressure promotes "silent" aseismic slip and low fault coupling prior to the main instability. The dependence on fluid pressure remains to be determined.**
- **Slip behavior and foreshock sequences depend on fault conditions.**
- **The energy dissipated prior to the earthquake seems to scale with the co-seismic energy associated to the event.**
- **Study of energy dissipation during induced seismicity can bring major insights to earthquake physics**

6- References

-Passelègue, F. X., et al., Influence of Fault Strength on Precursory Processes During Laboratory Earthquakes. Geophys. Mon. (2017)
-Summers, R., Byerlee, J.D., Summary of results of frictional sliding studies at confining pressures up to 6.98 kb. in selected rock materials., U.S. Geol. Surv. Open File Rep (1977)
-Proctor, B., Lockner, D.A., Pseudotachylyte increases the post-slip strength of faults. Geology (2016)
-Lockner, D.A., et al. The transition from frictional sliding to shear melting in laboratory stick-slip experiments., Geophys. Mon. (2017)
-Socquet, A., et al., An 8-month slow slip event triggers progressive nucleation of the 2014 Chile megathrust. Geophys. Res. Lett. (2017)
-Kato, A., et al., Propagation of Slow Slip Leading Up to the 2011 Mw 9.0 Tohoku-Oki Earthquake. Science (2012)

SCCER SoE
SWISS COMPETENCE CENTER for ENERGY RESEARCH
SUPPLY of ELECTRICITY

SCCER-SoE Annual Conference 2018

In cooperation with the CTI
Energy
Swiss Competence Centers for Energy Research
Schweizerische Eidgenossenschaft
Confédération suisse
Confederazione Svizzera
Confederaziun svizra
Swiss Confederation
Commission for Technology and Innovation CTI

Blocking probability at spillway inlets under driftwood impact

Paloma Furlan, M. Pfister, J. Matos and A.J. Schleiss*
**corresponding author: paloma.furlan@epfl.ch*

Introduction

Dam safety is strongly linked to the probability of occurrence of large floods. **Floods can transport large wood** (LW) into reservoirs and towards water release structures as spillways (Fig. 1 and 2).

For a better assessment of the related risk, the behaviour of LW in contact with hydraulic structures has to be quantified. Thus, the understanding of **LW blockage** process at spillways is important for **safety evaluations of dams**.

Figure 1: Picture of Oroville Dam, USA. (www.sacbee.com)

Figure 2: Picture of Yazagyo Dam, Myanmar. (www.thutatuam.net)

The present research project aims to describe and quantify systematically the **influence of LW characteristics** on the blocking process and the **effects a blockage** can have on the rating curve of an ogee crested spillway with piers.

Methodology and experiments

A physical model was designed and constructed in the facilities of LCH (Fig 3). An ogee crested spillway with round nose piers was chosen as it is a widely used structure and has a great ability to pass floods.

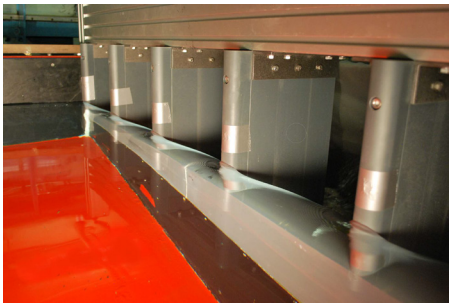

Figure 3: Upstream picture of the experimental facility at LCH

Experiments include different configurations tested, always having a reservoir approach.

Parameters

Blockage probabilities are estimated by varying the following parameters:

- **Diameter and length** of stems;
- **Stem density**;
- Spillway **bay width;**
- **Hydraulic head** at the spillway crest.

Different scenarios include **individual** stems or **groups**.

Additionally, **head increase** due to large wood blocked at the spillway inlet is investigated to understand the effect of a LW blockage.

Preliminary results

How can interactions between stems influence the blockage process at a spillway inlet? Does the amount of stems reaching a structure affect the blockage process? These questions were approached by systematically increasing the number of supplied stems and estimating blockage. Experiments have been concluded and the analysis is ongoing.

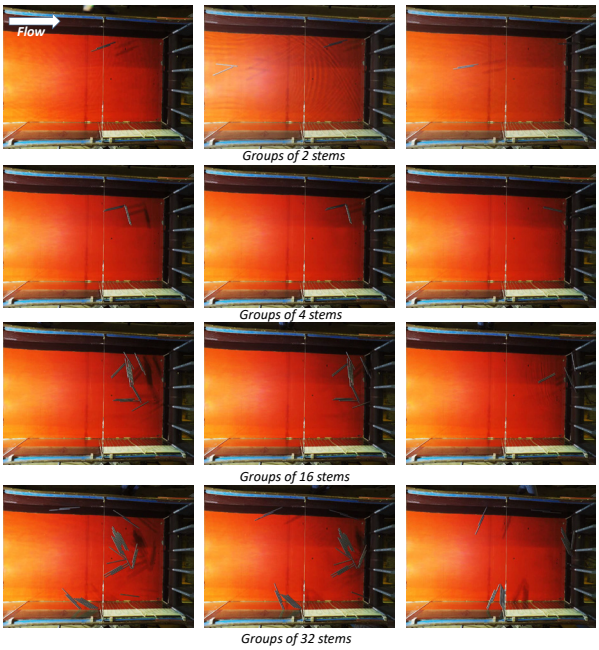

Figure 4: Pictures of blocking probability experiments for varied group sizes

Conclusions

Blocking probabilities were linked to the number of stems travelling towards the structure as a function of the hydraulic head and the length of stems.

For groups up to 4 stems, blocking probabilities increase as the size of the group increases. In some experiments, blockage probability of 4 stems is twice the value than for a single stem.

Acknowledgments

This research project is developed in the scope of the Ph.D. thesis by Paloma Furlan under the joint IST-EPFL doctoral program H2Doc. It is funded by the Portuguese Foundation for Science and Technology, LCH-EPFL and EDF.

Outcomes:

Furlan P, Pfister M, Matos J, Amado C, and Schleiss A.J (2018) "Experimental repetitions and blockage of large stems at ogee crested spillways with piers", *Journal of Hydraulic Research*, doi: 10.1080/00221686.2018.1478897

Furlan P, Pfister M, Matos J, and Schleiss A.J (2018) "Influence of density of large stems on the blocking probability at spillways". Daniel Bung, Blake Tullis, *7th IAHR International Symposium on Hydraulic Structures*, Aachen, Germany, 15-18 May. doi: 10.15142/T3664S

Furlan P, Pfister M, Matos J, and Schleiss A.J (2017) "Entrainement de bois flottant dans un déversoir a crête standard avec piliers: Influence des caractéristiques de bois flottant en probabilités de blocage" *Colloque CFBR-SHF*, Chambéry, France, 29-30 novembre 2017. p. 42-49. DOI : 10.24346/cfbr_shf_colloque2017_a04.

SCCER SoE
SWISS COMPETENCE CENTER for ENERGY RESEARCH
SUPPLY of ELECTRICITY

SCCER-SoE Annual Conference 2018

ETH zürich
VAW Laboratory of Hydraulics, Hydrology and Glaciology

Supported by:
Schweizerische Eidgenossenschaft
Confédération suisse
Confederazione Svizzera
Confederaziun svizra
Swiss Confederation
Innosuisse – Swiss Innovation Agency

Spatial Impulse Wave Generation and Propagation

Eva Sauter, Frederic Evers, Helge Fuchs, Robert Boes

Introduction

Gravity-driven mass movements may generate massive water waves, so-called impulse waves. As part of this thesis, further research is done on the spatial wave generation and propagation by conducting experiments. Besides landslides of small impacts and their underwater depositions, also the effect of slide density as well as of water body geometries are examined.

Background

Computation of wave characteristics usually considers two extreme cases: 2D or 3D. For calculation the impulse product parameter P (Heller & Hager, 2010) is of high significance. Wave characteristics increase with increasing P.

$$P = F\, M^{0.5}\, S^{0.25}\, \cos^{0.5} 6 / 7\, \alpha$$

Evers (2017) developed equations to compute the wave characteristics a_{c1}, a_{t1}, a_{c2}, H_1 and T_1 for varying propagation angles γ and radial distances r (s. Fig. 1). The equations are based on 74 3D tests with material of the same density ($\rho_s > \rho_w$) and for different experimental set-ups.

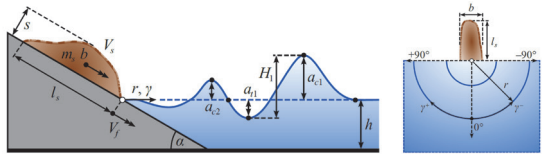

Fig. 1: Visualization of governing parameters and wave features for spatial impulse wave generation (Evers, 2017)

The wave decay is strongly dependent on the water body geometry. Heller and Spinneken (2015) showed that 3D waves decay faster and propagate slower than 2D waves. Furthermore, Heller et al. (2016) determined numerically for geometries with diverging angles θ, that wave amplitudes along the slide propagation angle lie approximately halfway between 2D and 3D for θ = 7.5° and are practically the same for θ = 45°.

Methodology

Experiments were conducted in a test basin of 8.0 m x 4.5 m and 0.75 m height (s. Fig. 2). Slide velocities were determined by dry tests, using laser distance sensors for measuring. Wave amplitudes were measured with ultrasonic devices (USD). 12 USD were placed in radial distances between 1.6 and 2.8 m on three axes: 0°, 35° and 70°. Overall, 18 different experimental set-ups were tested and evaluated. The considered parameter range can be seen in Table 1. Underwater depositions were measured with a grid on the basin bottom of 5 cm x 5 cm and registered by underwater camera (GoPro).

Tab. 1: Applied parameter range for conducted experiments

Parameter	h [m]	α [°]	Δz_{sc} [m]	b [m]	s_0 [m]	V_s [l]
Landslides	0.20 - 0.65	30 - 90	0.65 - 1.20	0.25 - 0.50	0.047 - 0.05	7.5 - 15
Avalanches	0.20 - 0.65	30 - 60	0.65 - 1.20	0.25 - 0.50	0.05	7.5 - 15

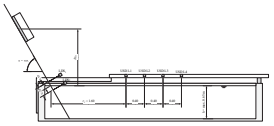

Fig. 2: Test basin, cut along the slide propagation axis (γ = 0°)

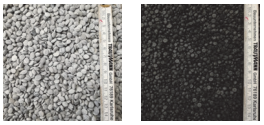

Fig. 3: Replacement materials, 87% $BaSO_4$, 3% PP, ρ_s = 1'338 kg/m³ (right), 100% PP, ρ_s = 573 kg/m³ (left)

Results and Discussion

Landslides and avalanches of small impact

Measured amplitudes were compared with predicted values according to Evers (2017) and show a relatively poor agreement (s. Fig. 4). Thus, wave amplitudes for small impulses are overestimated by approximately a factor of 2. Largest deviations occur for small amplitudes. It must be noted that for small amplitudes the applied measurement technology meets its limits due to accuracy.

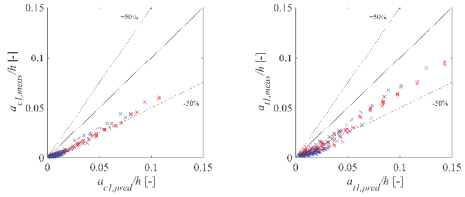

Fig. 4: Comparison of measured amplitudes (first wave crest a_{c1} and trough a_{t1}) with predicted values according to Evers (2017) [red: landslides, blue: avalanches]

Effect of water body geometry

Experiments from earlier work (Evers, 2017) were additionally analyzed. Different geometries with diverging angles were under estimation (θ= 10°, 20° and 30°) and compared to a 3D test (θ= 90°). All tests are within similar parameter range (0.67 ≤P≤ 0.82). The wave shows similar behavior in decay as Heller et al. (2016) determined by numerical modelling. For θ= 30° the wave amplitudes are already close to those for 3D test (s. Fig. 5).

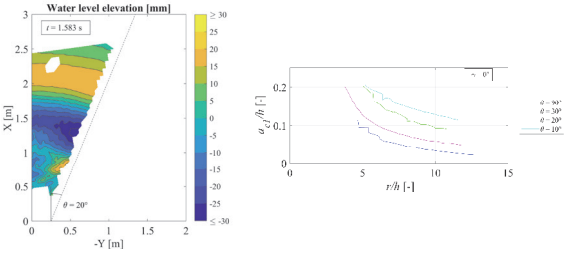

Fig. 5: Spatial wave propagation for t = 1.583 s and θ = 20° (left) and wave decay of the first wave crest along the slide propagation angle for θ = 90°, 30°, 20° and 10° (right)

Conclusion

The applied parameter range of the experiments lies mainly out of the range of Evers (2017). Further research and more experiments will be needed on spatial propagation of impulse waves to approve the 3D computation for small impacts. The estimated effect of the water body geometry shows the expected behavior. As it was analyzed only for slide impact angles of 30°, further analysis of experiments needs to be done to confirm.

References

Evers, F. M., 2017. Spatial Propagation of Landslides Generated Impulse Waves. Zurich: ETH Zurich.

Heller, V., Bruggemann, M., Spinneken, J. & Rogers, B. D., 2016. Composite modelling of subaerial landslide-tsunamis in different water body geometries and novel insight into slide and wave kinematic. *Coastal Engineering*, 109

Heller, V. & Hager, W. H., 2010. Impulse Product Parameter in Landslide Generated Impulse Waves. *Journal of Waterway, Port, Coastal, and Ocean Engineering*, 136(3).

Heller, V. & Spinneken, J., 2015. On the effect of the water body geometry on landslide-tsunamis: Physical insight from laboratory tests and 2D to 3D wave parameter transformation. *Coastal Engineering*, 104.

SCCER SoE
SWISS COMPETENCE CENTER for ENERGY RESEARCH
SUPPLY of ELECTRICITY

SCCER-SoE Annual Conference 2018

ETH zürich
VAW Laboratory of Hydraulics, Hydrology and Glaciology

Supported by:
Schweizerische Eidgenossenschaft
Confédération suisse
Confederazione Svizzera
Confederaziun svizra
Swiss Confederation
Innosuisse – Swiss Innovation Agency

Impulse waves: run-up behavior and overtopping at dam structures

Fabian Küttel, Frederic Evers, David Vetsch, Robert Boes

Introduction

Waves generated by impulse of a rockfall, landslide, avalanches or earthquakes will lead to water waves in reservoirs, which run-up at the coast or at dam structures up to several meters. In this Master's thesis a numerical model is implemented in OpenFOAM for the run-up and overtopping at dam structures and compared to given experimental results.

Background

The behavior of an impulse is divided in three stages (Fig. 1, top). For the given topic, the relevant ones are, the wave propagation (stage 2) and the run-up behavior (stage 3). In the propagation stage the solitary wave with its typical profile, a single peak and no wave trough (Fig. 1, bottom), builds up and propagates towards the dam by holding the same shape. Solitary waves illustrate the extreme case for overtopping. Therefore it is used to analyze the structural safety (especially the erosion) of the dam (Heller and Hager 2011).

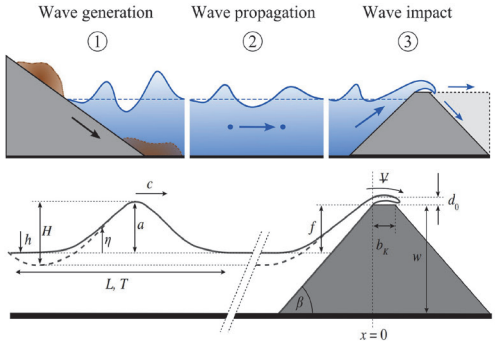

Fig. 1: Top: Impulse wave stages in a reservoir (Evers 2017). Bottom: Parameter definition for solitary wave (solid line) and overtopping at dam structure (Kobel et al. 2017).

In a previous, study experimental results were generated in a rectangular channel at the VAW at ETH Zurich (Kobel et al. 2017). The channel had a length of 11 m, a width of 0.5 m and a the end a dam with a height of 0.3 m. The waves are generated by an piston-type wave generator with a relative wave amplitude of $\varepsilon = a / h$.

Methodology

The numerical model is building up by using the open source program OpenFOAM. First the solitary wave behavior has to be proved in a simple numerical channel model, researched by the behavior of the wave amplitude a and the internal velocity field (Munk 1949). To find the final model, the boundary conditions were varied and different wave generator methods were used. Finally the wave generator method by Grimshaw and a rough wall at the bottom is implemented. The prior model, used for stage 2, was modified for the overtopping part (wave stage 3) by implementing the dam and using seven single blocks (Fig. 2) within a particular cell size of 0.5 mm in all directions.

Fig. 2: Numerical model for overtopping with seven blocks (dotted line).

The recorded parameters are the overtopping flux $Q(t)$, the volume $\forall$ and the maximum overtopping depth $d_0(t)$. The used input parameter range is shown in Table 1.

Results

Before the solitary wave spills over, the internal velocity field is checked at 1.5 m before the dam structure in the non influenced area (Fig. 3). During the overtopping a comparison of the water surface shape is done (Fig. 4).

Tab. 1: Parameter range

Parameter			min	max
Still water depth	h	[m]	0.20	0.30
relative wave amplitude	ε	[-]	0.20	0.70
dam height	w	[m]	0.30	
crest width	b_k	[m]	0.02	0.16
front face angle	β	[°]	18.4	90

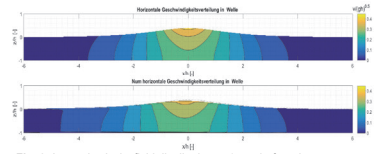

Fig. 3: Internal velocity field distribution at 1.5 m before dam.

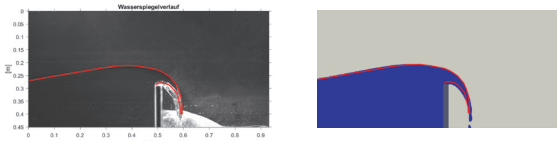

Fig. 4: Qualitative comparison of water surface between the experimental and the numerical data. Initial parameters are: h = 0.25 m; a = 0.075 m; b_k = 0.02 m; w = 0.30m.

All simulations are normalized for the overtopping volume $\forall$ and for the maximum overtopping depth d_0 according to Kobel et al. (2017) (Fig. 1 and 5).

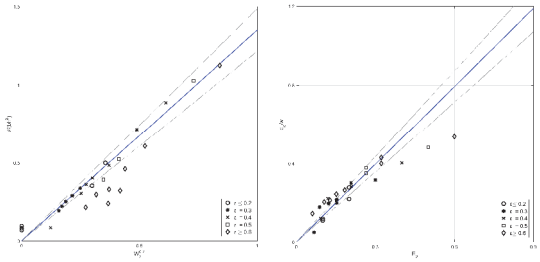

Fig. 5: Left: Relative overtopping volume $\forall$ and right the relative maximum overtopping depth d_0. The grey - dotted line shows the +/- 10% deviation.

Conclusions

In general, a relative wave amplitude higher than 0.5 results in an internal velocity profile difference >10% of the solitary wave and the wave amplitude is to small. For relative amplitudes between $0.2 \leq \varepsilon \leq 0.4$ the received data produce reasonable results. For $\varepsilon \geq 0.5$ the overtopping volume is significantly to low. In case the initial water table has the same level as the dam crest ($h = w$), for every relative amplitude, the overtopping depth is too low.
Relating to the reality, the most expected wave amplitudes in reservoirs are $0.2 \leq \varepsilon \leq 0.4$ and can be calculated by the model.

References

Evers, F. M. (2017). Spatial Propagation of Landslide Generated Impulse Waves. *Dissertation* 24650, ETH Zurich, Zurich.

Heller, V. and Hager, W.H. (2011). Wave types of landslide generated impulse waves. *Ocean Eng.*, 38(4), 630-640.

Kobel, J.; Evers, F. M. and Hager, W.H. (2017). Impulse wave overtopping at rigid dam structures. *Journal of Hydraulic Engineering*.

Munk, W.H. (1949). The solitary wave theory and its applications to surf problems. *Ann. N.Y. Acad. Sci.*, 51:376-424.

SCCER SoE
SWISS COMPETENCE CENTER for ENERGY RESEARCH
SUPPLY of ELECTRICITY

SCCER-SoE Annual Conference 2018

ETH zürich
VAW Laboratory of Hydraulics, Hydrology and Glaciology

Supported by:
Schweizerische Eidgenossenschaft
Confédération suisse
Confederazione Svizzera
Confederaziun svizra
Swiss Confederation
Innosuisse – Swiss Innovation Agency

Wave generation by submarine mass failures

Nina Landolt, Frederic Evers, Helge Fuchs, Robert Boes

Introduction

Historic events have shown a danger potential in Switzerland regarding tsunamis caused by landslides [1]. Popular examples are Lake Geneva in 563 AD [2] and Lake Lucerne 1601 [3], when subaqueous landslides induced waves of several meters. In this Master's thesis, physical 2D experiments of underwater landslides were performed. The aim is to improve the understanding of the underlying processes of wave generation due to submarine mass failures, as well as the generation of a dataset for the calibration of numerical models.

Background

Fig. 1 shows a wave with its principle parameters. The parameters are required to mathematically classify a wave [4].

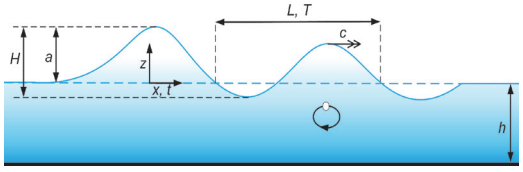

Fig. 1: Definition sketch of principal wave parameters

- c [m/s] = Wave celerity
- h [m] = Still water depth
- L [m] = Wave length
- T [s] = Wave period
- H [m] = Wave height
- a [m] = Wave amplitude

Methodology

Experimental Setup

Fig. 2 shows the setup of the physical 2D model of a channel with a width of 0.5 m, a depth of 1 m and a length of 11 m. Seven ultrasonic device sensors (UDS) are fixed at a distance of Δx = 0.8 m, to capture the water level change.

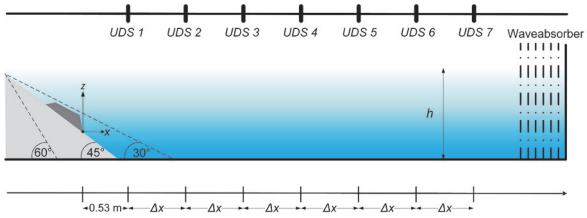

Fig. 2: Definition sketch of experimental setup

Experiments

Two series of experiments were conducted:

1) Comparison of granular and rigid slides with slide plane angles α = 30°, 45° and 60° and still water depths h = 0.7, 0.8 m and 0.87 m
2) Velocity field examinations with Particle Image Velocimetry (PIV). Velocity vectors were identified by cross-correlating images acquired between two laser pulses.
   With the measurements of the UDS, the wave amplitudes as well as the time periods were evaluated. The rigid and granular slides were compared visually as well as quantitatively on the basis of maximal amplitudes and time periods.

Results and Discussion

Fig. 3 shows an experiment conducted in the channel at VAW. Below, important experiment parameters are listed.

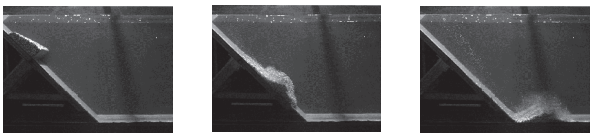

Fig. 3: Image series of experiment in channel d_g = 8 mm, α = 45°a, h = 0.8 m, m_s = 12.3 kg

- α [°] = Slide plane angle
- d_g [mm] = Particle size
- m_s [kg] = Slide mass
- ρ_s [$\frac{kg}{m^3}$] = Slide density
- $\frac{\eta}{h}$ [−] = Water level displacement
- t [s] = Time
- g [$\frac{m}{s^2}$] = Gravit. acceleration, 9.81 $\frac{m}{s^2}$

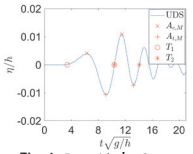

Fig. 4: Exp. with d_g = 8 mm α = 45°, h = 0.8 m, m_s = 12.3 kg, UDS # 3. First wave crest and trough ($A_{c,M}$, $A_{t,M}$) and time periods (T_1 ,T_2) of granular slide.

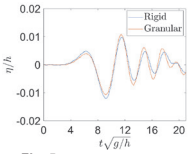

Fig. 5: Comparison between granular (d_g = 8 mm) and rigid slides, α = 45°, h = 0.8 m, m_s = 12.3 kg, UDS # 3

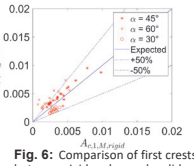

Fig. 6: Comparison of first crests between rigid and granular slides. 14 experiments are shown (7 comparison), with 7 UDS each.

The comparison of the conducted experiments (fig. 6) shows differences in max. amplitudes up to 50% for slide plane angles of 45° and 30° and over 100% for an angle of 60°. Fig. 7 and 8 show the velocity fields of slides with α = 60° at t = 0.8 s. The quality of the vector field increases with higher water velocities. It can be seen that for an angle of 60°, the granular slide generates higher velocities.

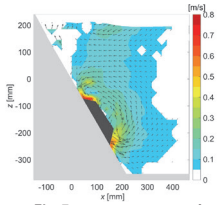

Fig. 7: Rigid slide with α = 60°, h = 0.8 m, m_s = 12.3 kg, t = 0.8 s

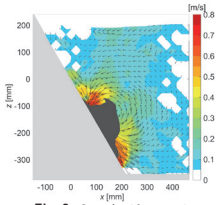

Fig. 8: Granular (d_g = 8 mm) slide with α = 60°, h = 0.8 m, m_s = 12.3 kg, t = 0.8 s

Conclusion

Amplitudes of granular slides are generally higher compared to rigid slides when α exceeds 45° and lower for smaller angles. A direct conversion between granular and rigid slides proves to be difficult. Additionally, lower bank inclinations (α < 30°) should be considered in further experiments. Particle Image Velocimetry can be used to compare velocity fields and visually examine the wave generation process. However, air trapped in the slide bodies often leads to incorrect velocity vector detection. Therefore, the experiment approach and evaluation processes can still be improved.

References

[1] Strupler, M., Danciu, L., Hilbe, M., Kremer, K., Anselmetti, F. S., Strasser and M., Wiemer, S. (2018): A subaqueous hazard map for earthquake-triggered landslides in Lake Zurich, Switzerland, *Natural Hazards* 90: 51 – 78.
[2] Schnellmann, M., Anselmetti, F.S., Giardini, D., McKenzie, J.A. and Ward, S.N. (2002): Prehistoric earthquake history revealed by lacustrine slump deposits, *Geology* 30, 1131 – 1134.
[3] Kremer, K., Simpson, G. and Girardclos, S. (2012): Giant Lake Geneva tsunami in AD 563, *Nature Geoscience* 5.
[4] Heller, V., Hager, W.H. and Minor, H.-E. (2009): Landslide generated impulse waves in reservoirs: Basics and computation, *VAW-Mitteilung* 211, Versuchsanstalt für Wasserbau, Hydrologie und Glaziologie (VAW), R. Boes, Ed., ETH Zürich.

SCCER SoE
SWISS COMPETENCE CENTER for ENERGY RESEARCH
SUPPLY of ELECTRICITY

SCCER-SoE Annual Conference 2018

Supported by:
Schweizerische Eidgenossenschaft
Confédération suisse
Confederazione Svizzera
Confederaziun svizra
Swiss Confederation
Innosuisse – Swiss Innovation Agency

Influence of tunnel slope on air demand and flow conditions of bottom outlets

Alexander Williams, Benjamin Hohermuth, Lukas Schmocker, Robert Boes

Introduction and Motivation

Due to the high velocities in bottom outlets, significant negative pressures may occur. To better understand these processes, the different flow conditions as well as the air demand in horizontal and inclined tunnels were analyzed. The overall goal was ensure controlled flow conditions and to minimize negative pressures thereby reduce the danger of cavitation.

Experimental setup and measurements

The experimental analysis has been carried out on a 20 meter long channel (Fig. 1). It consisted of all relevant elements of a bottom outlet. The energy head at the gate and the gate opening were varied to investigate different Froude numbers at the vena contracta. Orifice plates of different size were used to vary the loss coefficient of the air vent.

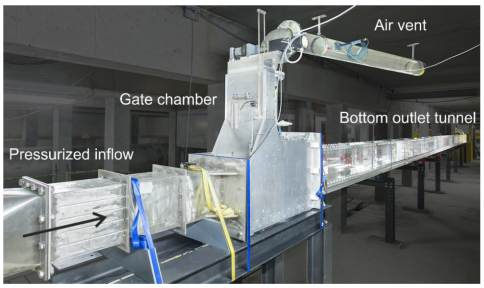

***Fig. 1**: Hydraulic scale model at Laboratory of Hydraulics, Hydrology and Glaciology (VAW).*

To investigate the influence of the tunnel slope, the tunnel was changed from horizontal (0%) to a 4% inclination.
Although several flow conditions were observed, the focus of the work was placed on the transition from free surface to slugflow. This transition is the most violent and poses the largest risk of cavitation. Hence, it has to be avoided in bottom outlets.

Results of the flow conditions

With the experimental setup the formation slugflow could be analyzed (Fig. 2). The observations showed that a strong counter-current air flow is responsible for the formation of slugs. Such a counter-current air flow is induced by large water flow velocities and large loss coefficients of the air vent.

***Fig. 2:** A slug photographed in the hydraulic scale model. Flow direction from left to right.*

To analyse slug formation, β_{total} was defined as the total air inflow (though the air vent and from the downstream tunnel end) divided by the water inflow into the system. Furthermore, slugflow depends on the water pressure upstream of the gate P_o and the minimal air pressure $P_{a,min}$ downstream of the gate chamber. These findings resulted in the design diagram shown in Fig. 3.

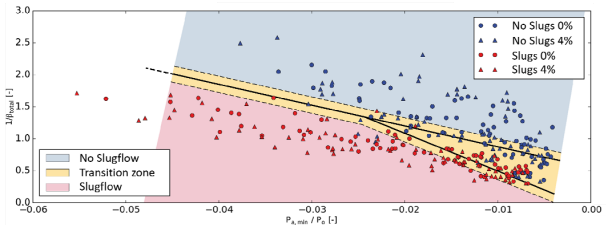

***Fig. 3:** The resulting correlation of the research results for the identification of slugflow in bottom outlets*

Figure 3 allows to delineate slugflow from free surface flow. The total air discharge and the minimal air pressure have a decisive influence on the formation of slugs while the tunnel slope has no significant effect.

Results on air demand

Air demand

Information on the air demand in a bottom outlet are essential for dimensioning the air vent and for calculating the mixed water depth. Measurements have shown, that the influence of the tunnel slope is small. However, it still has some influence on the water depth, especially further downstream of the gate as can be seen in Fig. 4. Due to the higher velocity in the inclined channel, the mixed water depth lies below the one of the horizontal channel.

Backwater curve

In order to understand how the mixed flow depth propagates in bottom outlets, the classic backwater curve was calculated. Knowledge on the water level is needed to avoid the transition to pressurized flow, i.e., flow chocking. Considering Fig. 5 it becomes apparent that this approach returns values only for clear-water depth as it does not account for the entrained air. Accordingly, the influence of the air, i.e., flow bulking, has to be taken into account. Therefore, an empirical approach by Speerli and Hager (2000)[1] has been adopted. This returns a calculated mixture flow depth also shown in Fig. 5.

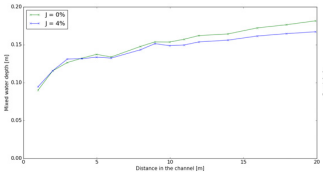

***Fig. 4:** Measured mixture flow depth h_{90} for the horizontal (0%) and the inclined (4%) channel.*

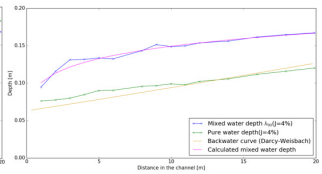

***Fig. 5:** Backwater curve calculation for the clear-water and mixture flow depth.*

Conclusions

Bottom outlets are vital elements for the security of high-head dams. The measurements have shown that the inclination of a bottom outlet tunnel has slight, but not essential influence on the flow conditions and the air demand.
To prevent slugflow or cavitation in bottom outlets, the air vent must be dimensioned large enough.

[1] J. Speerli and W. H. Hager (2000). Air-water flow in bottom outlets. *Canadian Journal of Civil Engineering.*

SCCER SoE
SWISS COMPETENCE CENTER for ENERGY RESEARCH
SUPPLY of ELECTRICITY

SCCER-SoE Annual Conference 2018

Supported by:
Schweizerische Eidgenossenschaft
Confédération suisse
Confederazione Svizzera
Confederaziun svizra
Swiss Confederation
Innosuisse – Swiss Innovation Agency

Numerical Simulations of Two-Phase Flow in Bottom Outlets

Matthias Bürgler, Benjamin Hohermuth, David Vetsch, Robert Boes

1 Introduction

Bottom outlets are key safety features of high-head reservoirs. Air vents are installed downstream of the gate (Fig. 1) to limit negative pressures and potential problems with cavitation. So far the air discharge $Q_{a,o}$ is calculated based on empirical equations which scatter over one order of magnitude, thus prohibiting a coherent design of air vents. The use of numerical models for air discharge simulations requires accurate modelling of two-phase flow in bottom outlets, currently posing the main limitation.

2 Background

The review of literature, e.g. [1], and previous studies at the Laboratory of Hydraulics, Hydrology and Glaciology (VAW) indicate that Eulerian one-fluid models overestimate $Q_{a,o}$ in bottom outlets. So far, the overestimation was blamed on the description of two-phase flow with one Reynolds averaged Navier-Stokes equation and volume-weighted fluid properties. The more complex Eulerian two-fluid model solves the velocity field of each phase separately [2]. Thus, it results in a less diffusive momentum transfer at the air-water interface and is expected to improve predictions of $Q_{a,o}$.

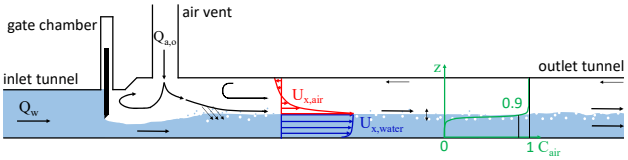

Fig. 1: The high-speed water jet drags a significant amount of air towards the tunnel outlet. Additionally, air is entrained into the water phase resulting an air concentration profile.

However, recent findings in literature suggest that k-ε turbulence models overestimate air-side turbulence near the interface [3], affecting the simulation of air velocities in both one- and two-fluid models. In [3], dampening of air-side turbulence at the air-water interface is proposed. This is achieved by introducing an additional source term in the transport equation of the dissipation rate ε_a. In this study, a two-fluid model in combination with an improved turbulence model was implemented in OpenFOAM and was applied for air discharge simulations for the first time.

3 Methodology

Numerical simulations of two-phase flow in a bottom outlet model at VAW were performed using a one- and two-fluid model in OpenFOAM. The one-fluid model is implemented with a realizable k-ε turbulence model. The two-fluid model is combined with an improved standard k-ε model, whereby the air-side turbulence is dampened in proximity of the interface, following the approach of [3]. The idea is to force the dissipation rate ε_a at the interface to a "wall-like" value by adding the source term $\mathcal{R}_a^{int}$ in (1) to the r.h.s. of the transport equation of ε_a.

$$\mathcal{R}_a^{int} = A\, C_2 \alpha_a \rho_a \frac{v_a^2 k_a}{\delta^4} \qquad (1)$$

The formulation of interface indicator field A given in (2) was developed in this thesis and confines the dampening of turbulence to the region of the air-water interface at 90% air concentration ($\alpha_a \approx 0.9$).

$$A = \max\left[\exp\left(\frac{(0.92-\alpha_a)^2}{2 \cdot 0.02^2}\right) 0.001, 0\right] \qquad (2)$$

4 Results

The results of the one- and the two-fluid model are compared to data from hydraulic model tests.

Velocity profiles & air discharge

The velocity profiles of both models are displayed in Fig. 2. The experimental data serves as rough reference (±15%) for the velocity in the water-air mixture.
The two-fluid model results in smaller velocities than the one-fluid model for $z > 0.1$ m, i.e., in the air-phase. Consequently, the two-fluid model with the improved turbulence model predicts the measured $Q_{a,o}$ with an error of +6%, while the one-fluid model results in an overestimation of +44%.

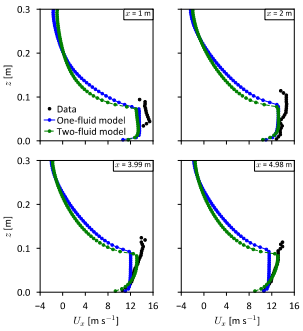

Fig. 2: Comparison of simulated velocities U_x and experimental data.

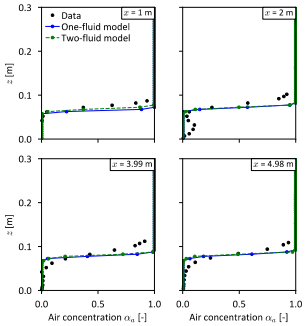

Fig. 3: Comparison of simulated and experimental air concentration profiles

Air concentrations

Both models result in a sharp air-water (Fig. 3) interface because air entrainment is not implemented in the numerical models. For the two-fluid model, predictions of air concentrations were improved by including turbulent dispersion on a sub-grid scale. However, this had a counter-active effect on turbulence dampening and $Q_{a,o}$ predictions.

5 Conclusions

Numerical simulations with one-fluid models and conventional k-ε turbulence models result in a significant overestimation of the air discharge $Q_{a,o}$ by 44%. With a two-fluid model in combination with an improved k-ε turbulence model that dampens turbulence at the air-water interface, the model performance was enhanced and the error in air discharge simulation was reduced to 6%. The measured air concentration profiles were not reproduced accurately by either model. Modelling air entrainment by means of turbulent dispersion in a two-fluid model had counter-active effects on the air discharge simulation and thus requires further research.

6 References

[1] Shamsai, A., & Soleymanzadeh, R. (2006). Numerical simulation of Air-Water flow in bottom outlet. *International Journal of Civil Engineering*, *4*(1), 14.
[2] Ishii, M., & Hibiki, T. (2011). Drift-flux model. In *Thermo-Fluid Dynamics of Two-Phase Flow* (pp. 361-395). Springer, New York, NY.
[3] Frederix, E. M. A., Mathur, A., Dovizio, D., Geurts, B. J., & Komen, E. M. J. (2018). Reynolds-averaged modeling of turbulence damping near a large-scale interface in two-phase flow. *Nuclear Engineering and Design*, *333*, 122-130.

SCCER SoE
SWISS COMPETENCE CENTER for ENERGY RESEARCH
SUPPLY of ELECTRICITY

SCCER-SoE Annual Conference 2018

RENOV Hydro

Supported by:
Schweizerische Eidgenossenschaft
Confédération suisse
Confederazione Svizzera
Confederaziun svizra
Swiss Confederation
Innosuisse – Swiss Innovation Agency

Les principaux vecteurs d'adaptation d'installations hydroélectriques de montagne en Suisse

Vincent Gaertner, Sabine Chamoun, Pedro Manso

Plateforme en Constructions Hydrauliques (PL-LCH), Ecole Polytechnique Fédérale de Lausanne (EPFL)
Corresponding author: vincent.gaertner@epfl.ch

Introduction

L'adaptation des installations hydroélectriques de montagne en Suisse représente un potentiel non-négligeable d'augmentation de la capacité de production d'énergie renouvelable. L'arrivée à échéance des concessions doit être l'occasion pour les exploitants de prévoir le renouvellement progressif des infrastructures et des équipements existants. En Suisse, ces démarches ont pour objectifs principaux d'augmenter la capacité de stockage pour **l'approvisionnement énergétique hivernal**, de créer de la **flexibilité** (pointe, services réseau) et d'assurer la conformité avec la **LEaux 2013** (Loi fédérale sur la protection des eaux).

Des réflexions peuvent également être menées sur les possibilités de densifier le parc hydroélectrique tout en garantissant une synergie entre les aménagements et une disponibilité accrue des installations (**redondance** systémique). Une vision intégrée du bassin versant est utilisée ici, indépendamment des concessions actuelles, des exploitants actuels ou de la structure d'actionnariat (vision SCCER, soit d'intérêt national).

Figure 1. Le barrage de la retenue de Ze Binnen, Canton du Valais *(crédit image: Vincent Gaertner)*

Démarche et vecteurs d'adaptation

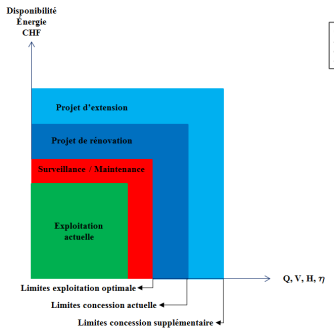

Figure 2. Potentiels d'adaptation d'un aménagement à différentes échelles

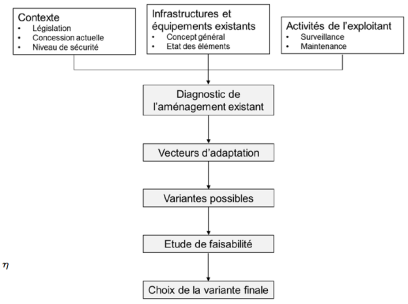

Figure 3. Démarche générale d'analyse pour la génération de variantes d'adaptation d'un aménagement existant

Génération de variantes

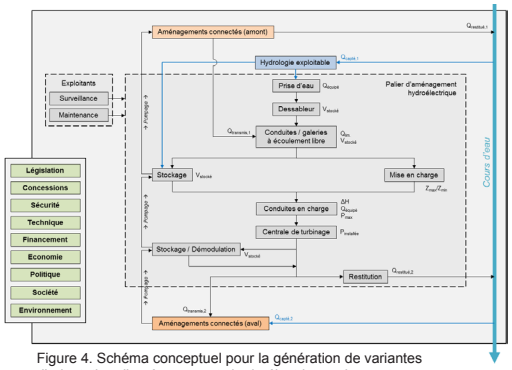

Figure 4. Schéma conceptuel pour la génération de variantes d'adaptation d'aménagements hydroélectriques de montagne

Cas d'étude et variantes d'adaptation

Le travail est effectué sur les aménagements GKW 1 et GKW 2 dans la Vallée des Conches en Valais. Il correspondent actuellement à deux palier distincts, le premier reliant la retenue de Kummenbord à la centrale de Heiligkreuz et le second reliant plusieurs sources et le bassin de Frid à la centrale de Neubrigg. La retenue de Ze Binnen (exploitée par FMV) pourrait, grâce à sa situation géographique, jouer un rôle central entre les systèmes actuellement déconnectés de cette vallée. Les variantes d'adaptation proposées ci-contre, qui visent à augmenter la flexibilité des aménagements, peuvent être caractérisées par l'échelle des interventions.

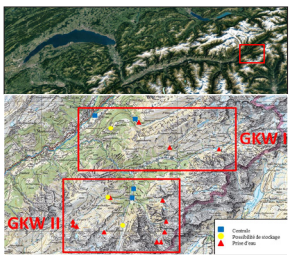

Figure 5. Situation et éléments principaux des aménagements GKW 1 et GKW 2

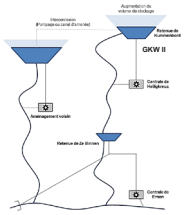

Figure 6. Echelle régionale à internationale. *Connexion avec la retenue d'un aménagement voisin.*

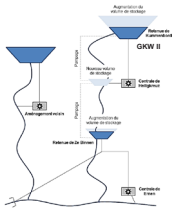

Figure 7. Echelle locale. *Augmentation de volumes de stockage et implantation de systèmes de pompage.*

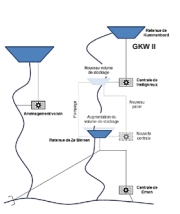

Figure 8. Echelle locale. *Création d'un nouveau palier reliant les aménagements GKW 1 et GKW 2.*

Discussion – Choix de l'échelle

En considérant que le choix de l'échelle d'analyse dépend principalement de la longueur du système d'adduction, de la topographie relative entre les retenues (canal d'amenée ou besoin de pompage) et des possibilités de stockage, l'estimation du prix de revient doit permettre d'évaluer la faisabilité économique des variantes d'augmentation de production hivernale générées et de déterminer l'échelle d'analyse optimale.

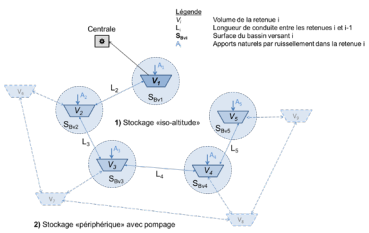

Figure 9. Schéma d'un réseau de stockage d'eau typique en montagne et ses paramètres

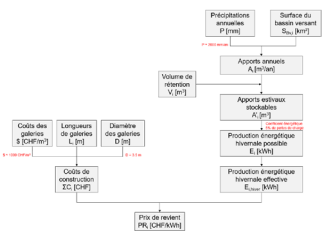

Figure 10. Démarche pour l'estimation des prix de revient en fonction des paramètres du réseau

Perspectives

Le travail en cours envisage l'établissement d'un cadre de réflexion permettant de générer de nouveaux plans d'affaires pour des interventions structurales sur des aménagements existants. L'interconnexion de systèmes ou l'élargissement des réseaux d'adduction pour profiter de nouveaux sites de stockage ("off-stream") seront difficilement justifiés par de simples augmentations d'énergie produite et requièrent des analyses plus fines des modes d'exploitation et des services rendus au réseau.

Références: Giovanni, M. (2018). *Rénovation d'aménagements hydroélectriques alpins*. Lausanne: Ecole Polytechnique Fédérale de Lausanne, Laboratoire de Constructions Hydrauliques.

SCCER SoE
SWISS COMPETENCE CENTER for ENERGY RESEARCH
SUPPLY of ELECTRICITY

SCCER-SoE Annual Conference 2018

RENOV Hydro

Supported by:
Schweizerische Eidgenossenschaft
Confédération suisse
Confederazione Svizzera
Confederaziun svizra
Swiss Confederation
Innosuisse – Swiss Innovation Agency

Valorisation des mesures de mitigation des éclusées en systèmes complexes : quelle échelle spatiale privilégier ?

groupe e
FMV

Mathieu Barnoud, Sabine Chamoun, Pedro Manso

Plateforme en constructions hydrauliques (PL-LCH), Ecole polytechnique fédérale de Lausanne (EPFL), Lausanne.
contact : mathieu.barnoud@epfl.ch

EPFL ECOLE POLYTECHNIQUE FÉDÉRALE DE LAUSANNE

Motivation

Les détenteurs de centrales hydroélectriques existantes ont pour obligation de prendre, jusqu'à fin 2030, des mesures en matière de mitigation des éclusées d'après l'art. 83 de la loi fédérale sur la protection des eaux (LEaux). Cependant, selon la loi sur l'énergie (art. 15), la Société nationale pour l'exploitation du réseau à très haute tension (Swissgrid), en accord avec l'office fédéral de l'environnement (OFEV) et le canton concerné, rembourse les coûts des mesures prises en vertu de la LEaux. Il serait alors intéressant d'essayer de profiter de cette subvention pour proposer des mesures qui répondront aux exigences de la loi tout en améliorant les aménagements concernés.

Définition et méthodes d'évaluation des éclusées

Les éclusées désignent des variations quotidiennes du débit d'un cours d'eau, occasionnées par des centrales hydroélectriques fonctionnant par intermittence. En effet, lorsque la demande en courant est élevée, la centrale turbine un débit d'eau important et la restitution de cette eau accroît le débit en aval. Le phénomène inverse se produit lorsque la demande est faible. Meile (2011) propose deux paramètres pour caractériser les éclusées : l'amplitude de la fluctuation journalière du débit relative HP_1 et le gradient par rapport au temps HP_2 .

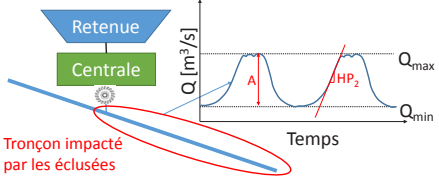

$$A = Q_{max,j} - Q_{min,j}$$

$$HP_{1,j} = \frac{A}{Q_{moyen,j}}$$

$$HP_{2,i} = \frac{Q_i - Q_{i-1}}{t_i - t_{i-1}}$$

Le calcul de ces indicateurs peut se faire avec les données publiques des stations hydrométriques de l'OFEV ou bien avec les données d'exploitation fournies par les exploitants.

En comparant ces deux types de données, il est possible de déterminer si un aménagement a un impact sur les éclusées telles que mesurées à l'aval par une station publique. Ici par exemple, l'aménagement de Mörel (VS) semble jouer un rôle dans les variations de débit mesurées à Brig. La distance à laquelle les mesures sont faites ne donnes pas toujours une estimation directe, due aux multiples apports intermédiaires

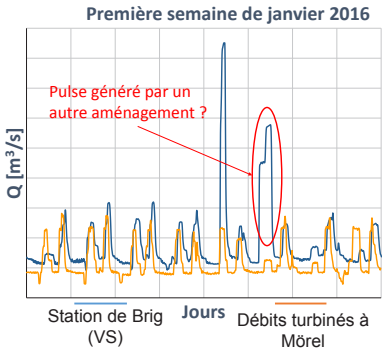

Exemples de méthode de mitigation des éclusées

Réduction du gradient des éclusées à l'aide d'un bassin de compensation.

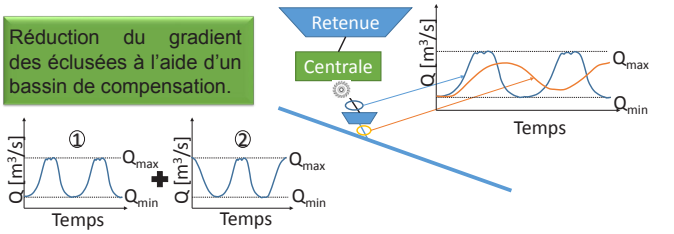

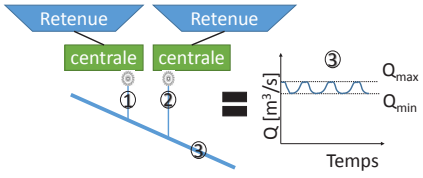

Réduction du gradient et de l'amplitude des éclusées par décalage du turbinage de deux centrales voisines.

Une autre méthode possible est le changement du programme de turbinage pour réduire l'amplitude et les gradients des éclusées. Cependant cette méthode entraine souvent des pertes de revenus.

Exemples de valorisation des mesures de mitigation à plusieurs échelles

A l'échelle d'un aménagement :
le bassin de compensation peut être utilisé à des fins de stockage ou de pompage sans modification de la concession.

A l'échelle de plusieurs aménagements :
Cas de la liaison Heiligkreuz-Ze binnen (VS). Les éclusées seraient supprimées par l'ajout d'un palier d'environ 100m de chute.

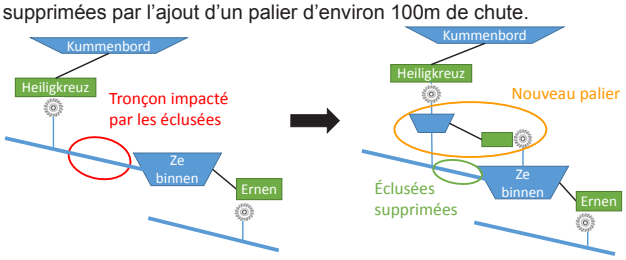

Travailler à l'échelle de plusieurs aménagements ouvre des possibilités intéressantes économiquement et énergétiquement.

Discussion

Analyser des données réelles pose plusieurs problèmes: quelles valeurs minimales et maximales du débit choisir? Quel gradient considérer ?

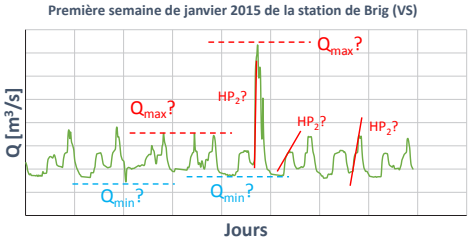

Le gradient est en général exprimé en m³/s/min car les exploitants peuvent fournir facilement les débits turbinés. Cependant, des valeurs en cm/min correspondent aux mesures réelles, permettent de prendre en compte la morphologie du cours d'eau et sont directement perceptibles part les parties concernées

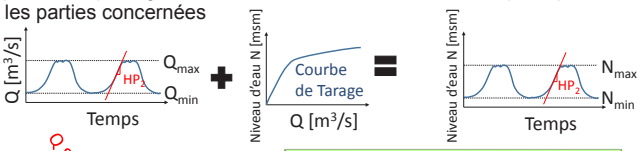

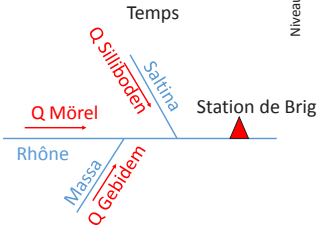

L'aménagement de Mörel n'est pas le seul à l'amont de la station de Brig. Des solutions de mitigation peuvent être trouvées avec les aménagements alimentant Mörel ou avec ceux des autres affluents du Rhône comme Gebidem ou Silliboden.

Perspective

Il ne reste que quelques années aux détenteurs de centrales hydroélectriques existantes pour prendre des mesures de mitigation des éclusées. Au lieu d'une obligation, ces mesures peuvent être perçues comme une opportunité d'amélioration en partie financée, et donc une chance. Pour cela, il sera sans doute nécessaire d'étudier les possibilités au-delà de l'échelle de l'aménagement et d'envisager des projets concernant plusieurs exploitants. A ce stade de réflexion sur le cas d'étude, nous estimons que la création d'un palier d'interconnexion de deux systèmes dans une seule cascade pourrait être éligible pour co-financement par Swissgrid dans le cadres des mesures de mitigation des éclusées.

Références

OFEV, « Assainissement des éclusées – Planification stratégique », 2012
OFEV, « Eclusées – mesures d'assainissement », 2017
OFEV , « Assainissement écologique des centrales hydrauliques existantes : Financement des mesures requises » , 2016
Meile. T, Boillat. J-L, Schleiss. A. J, Aquat sci (2011) 73:171-182 DOI 10.1007/s00027-010-0154-7